ACSNANO

www.acsnano.org

REVIEW

Photodynamic and Photothermal Therapies: Synergy Opportunities for Nanomedicine

Marta Overchuk, Robert A. Weersink, Brian C. Wilson, and Gang Zheng*

Cite This: *ACS Nano* 2023, 17, 7979–8003

Read Online

ACCESS | Metrics & More | Article Recommendations

ABSTRACT: Tumoricidal photodynamic (PDT) and photothermal (PTT) therapies harness light to eliminate cancer cells with spatiotemporal precision by either generating reactive oxygen species or increasing temperature. Great strides have been made in understanding biological effects of PDT and PTT at the cellular, vascular and tumor microenvironmental levels, as well as translating both modalities in the clinic. Emerging evidence suggests that PDT and PTT may synergize due to their different mechanisms of action, and their nonoverlapping toxicity profiles make such combination potentially efficacious. Moreover, PDT/PTT combinations have gained momentum in recent years due to the development of multimodal nanoplatforms that simultaneously incorporate photodynamically- and photothermally active agents. In this review, we discuss how combining PDT and PTT can address the limitations of each modality alone and enhance treatment safety and efficacy. We provide an overview of recent literature featuring dual PDT/PTT nanoparticles and analyze the strengths and limitations of various nanoparticle design strategies. We also detail how treatment sequence and dose may affect cellular states, tumor pathophysiology and drug delivery, ultimately shaping the treatment response. Lastly, we analyze common experimental design pitfalls that complicate preclinical assessment of PDT/PTT combinations and propose rational guidelines to elucidate the mechanisms underlying PDT/PTT interactions.

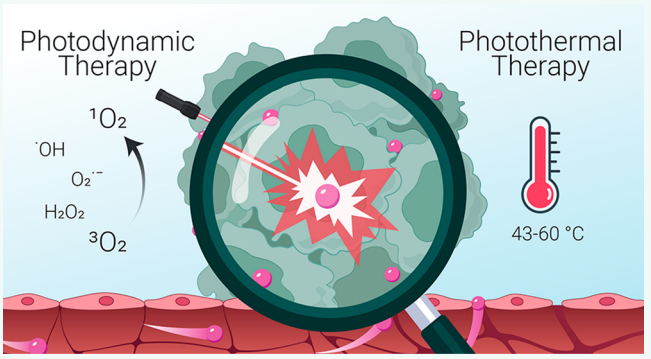

KEYWORDS: *photomedicine, cancer, photodynamic therapy, PDT, photothermal therapy, PTT, combination therapies, multimodal nanoparticles, drug delivery, theranostics*

INTRODUCTION

Phototherapies are rapidly evolving cancer treatment modalities that employ light of various wavelengths to induce photochemical or photothermal changes within a target tissue.[1] The two most common phototherapies include photodynamic (PDT) and photothermal (PTT) therapy, which utilize light and exogenous or endogenous absorbers to generate cytotoxic reactive oxygen species (ROS) or local temperature increase, respectively.[2] Due to their distinct mechanisms of action, PDT and PTT can complement mainstay cancer treatments. On the cellular level, both phototherapies have been shown to overcome chemotherapy resistance and compensatory signaling pathways.[3−8] On the tumor microenvironment level, PDT and PTT can modulate tumor perfusion, vascular and extracellular matrix permeability, which can be leveraged to enhance tumor drug delivery.[5,9−13] Additionally, PDT and PTT offer a greater degree of spatiotemporal control compared to systemic therapies, reducing off-target toxicities. Advances in endoscopic and fiberoptic light delivery techniques enable minimally invasive irradiation of various solid tumors, including in sensitive anatomic areas that may be inaccessible by surgery.[2,14−16] Finally, phototherapies employ nonionizing radiation and so reduce the risk of secondary cancer development compared to radiation therapy.

In a recent review, Wilson and Weersink compared and contrasted PDT and PTT as current and potential clinical techniques and discussed the factors to be considered in selecting which would be the preferred modality for several promising clinical applications.[1] Specifically, they analyzed the roles of PDT and PTT within the existing clinical paradigms for brain and prostate cancer. However, this article only briefly considered the combination of PDT and PTT and the enabling

Received: January 30, 2023
Accepted: April 10, 2023
Published: April 27, 2023

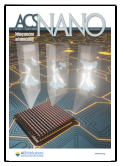

https://doi.org/10.1021/acsnano.3c00891
ACS Nano 2023, 17, 7979−8003

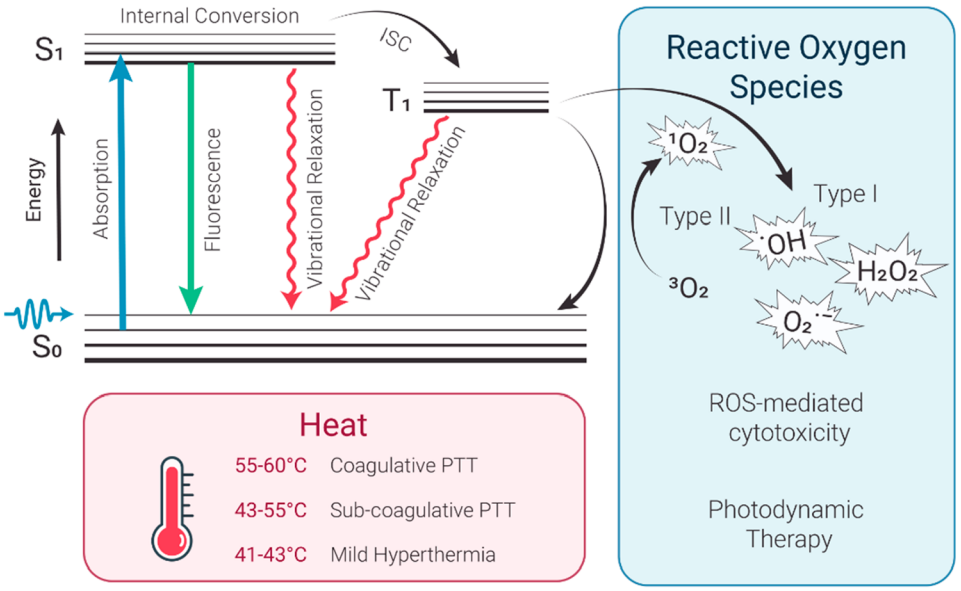

Figure 1. Simplified Jablonski diagram illustrating the photophysical and photochemical basis of PDT and PTT. S_0 − ground state, S_1 − excited singlet state, T_1 − excited triplet state, ISC − intersystem crossing.

role of nanoparticles in this combination. These topics are the focus of the present paper.

Here, we provide a brief overview of the fundamental principles of PDT and PTT, as well as delineate the areas in which their joint application has potential to synergistically enhance treatment safety and/or efficacy. The following sections will highlight critical mechanistic, translational and clinical considerations behind the PDT/PTT combination and examine their biological interplay. Next, we outline recent developments in nanomaterial design that facilitate the joint application of PDT and PTT. Finally, we discuss common experimental design limitations that riddle preclinical studies in this field and propose rational guidelines to help elucidate the mechanisms behind the PDT/PTT interactions. The goal of this article is to stimulate discussion around this emerging combination treatment and facilitate the development of tailored protocols that harness the strengths and minimize the limitations of each modality alone.

BASIC PRINCIPLES OF PDT AND PTT

PDT typically requires three principal components: light, a light-activatable compound (photosensitizer, PS) and, for many photosensitizers, also oxygen, which together undergo photodynamic reaction and produce cytotoxic ROS.[17,18] Incident light absorption by a PS molecule converts it from the ground state to a short-lived (~ns) excited singlet state, which then undergoes intersystem crossing to a relatively more stable (~ms) excited triplet state (Figure 1).[19] From this triplet state, photosensitizer molecules can return to the ground state by undergoing a type I or type II photodynamic reaction. In the former, activated PS transfers an electron to a substrate to form various ROS, including $O_2^{\bullet-}$, $HO^{\bullet}_2$.[20] During a type II reaction, the energy is transferred directly to molecular ground-state oxygen, creating highly reactive singlet oxygen, $^1O_2$.[17,19,20] The reactive species trigger many downstream biological events, including direct cytotoxicity, inflammation and vascular events.[17] Importantly, ROS have extremely short diffusion distance within cells and tissues (<50 nm),[21] so that photosensitizers generally need to be localized in a close proximity to the target structure. While most PS undergo one of the two classic oxygen-dependent photodynamic reactions (or their combination), it should be noted that there is an emerging class of oxygen-independent photosensitizers. For example, transition metal complexes, such as Ru (II) complexes, have been gaining momentum due to their longer triplet states compared to common porphyrin-based photosensitizers, facilitating both classic and oxygen-independent phototoxic pathways.[22,23] In terms of light dosimetry, PDT fluence rates are usually kept low (<200 mW/cm^2) to avoid the possible effects of tissue heating that would be an additional (and not well controlled) treatment factor that may increase the variance in treatment response. PDT-induced cell killing is dependent on the local photosensitizer concentration and local light fluence Ø, such that cell death does not occur unless the product of these values reaches some threshold value T_{PDT}.[1] Given the short ROS diffusion distance and localized light delivery, PDT often creates a sharp boundary between the necrotic regions that reached T_{PDT} dose and viable tissue regions.[24] Furthermore, since photosensitizers tend to localize within cancer cells, PDT has very mild effects on surrounding nerves[25−28] and extracellular matrix,[29] even when these are within the treatment field. This makes PDT suitable for tumors that are surrounded by crucial structures, including cancers of head and neck,[30] bladder,[31] esophagus,[32,33] lung,[34,35] prostate[36] and pancreas.[37]

Photothermal therapy (PTT) uses light (typically within the near-infrared, NIR, region) to raise tissue temperature and achieve local photocoagulation (Figure 1, bottom panel). PTT applies relatively high light powers to achieve subcoagulative (43−55 °C) or coagulative (55−100 °C) temperatures to induce rapid cell death via protein denaturation and cell membrane damage.[38,39] Milder heating regimens (41−43 °C) are classified as hyperthermia (Hx), which is not tumoricidal by itself unless applied for prolonged periods (>1 h).[40] Hx is not used clinically as a stand-alone modality but can be applied to increase the selectivity and efficacy of other modalities, such as chemotherapy or radiation therapy,[41] by inducing heat shock proteins and altering tumor perfusion and metabolic state.[42] Importantly, the temperature gradient created by PTT often has a hyperthermic zone extending beyond the frank coagulative

https://doi.org/10.1021/acsnano.3c00891
ACS Nano 2023, 17, 7979−8003

Table 1. Comparison of Key PDT and PTT Characteristics

	PDT	PTT	
Photoabsorber	Exogenous PS (or precursor)	Exogenous	Endogenous
Light power	<200 mW	200 mW−1 W	0.5−10 W
Irradiation method	Surface or interstitial	Surface or interstitial	Interstitial
Oxygen dependency	Oxygen is usually required	Oxygen not required	Oxygen not required
Primary mechanism	ROS generation	Temperature increase	Temperature increase
Treatment margin	Relatively sharp, defined by the localization of a PS	Largely defined by the localization of a photoabsorber	Gradient-like
Off-target effects	Cutaneous or ocular photosensitivity	Thermal damage of the surrounding tissues	Thermal damage of the surrounding tissues
Nerve preservation	Nerve-sparing	Potentially nerve-sparing, depends on the localization of a photoabsorber	Nonselective
Treatment monitoring and dosimetry	May involve monitoring PS uptake, oxygenation and light	Real-time temperature or tissue damage monitoring is preferred	Real-time temperature or tissue damage monitoring is required

boundary. PTT and Hx should also be distinguished from photothermal tissue ablation, which uses high-energy pulsed lasers to remove tissue from the surface. This modality is used to treat, for example, obstructive esophageal cancer[43,44] but its utility is limited due to safety concerns. Unlike PDT, which always requires a PS, PTT and Hx can be conducted with or without exogenous optical absorbers, although the use of external molecular or supramolecular agents is becoming increasingly common. Recent developments in PTT have utilized the insertion of thin optical fibers, with or without light-diffusing tips, into solid tumors for NIR light delivery, sometimes actively cooling the tip to avoid tissue charring and loss of light transmission. Ultrasound or magnetic resonance imaging (MRI) guidance enables precise fiber positioning, increasing treatment selectivity and safety. Laser interstitial thermal therapy has demonstrated promising results in prostate tumors[45] and colorectal carcinoma liver metastases,[46] particularly in patient cohorts with small tumors < ∼3 cm. Another clinically approved PTT application is treatment of brain tumors, including malignant primary, metastatic and non-malignant lesions.[47,48] Finally, several early phase clinical trials have explored the use of external photoabsorbers in combination with interstitial PTT with the goal of further improving selectivity and achieving heat confinement. This approach is exemplified by the use of gold nanoshells in prostate cancer patients[49,50] and indocyanine green (ICG) in patients with refractory advanced-stage metastatic breast cancer.[51]

Despite some technical similarities, there are several critical differences between the PDT and PTT that have significant clinical implications (Table 1). First, PDT effects are inherently more selective than PTT due to the dual selectivity of photosensitizer accumulation and light targeting. Additionally, as a nonthermal modality, PDT can preserve the surrounding collagen structures and nerves. Furthermore, due to the short ROS diffusion distance, PDT can be used to target infiltrative and nonresectable tumor components. However, for some photosensitizers, ocular and cutaneous photosensitizer accumulation may cause photosensitivity, complicating treatment logistics and compromise safety. Unlike PDT, PTT selectivity primarily relies on localized light delivery, inevitably creating a temperature gradient. The lack of heat confinement mechanisms results in thermal damage beyond the frank photocoagulation zone, increasing the risk of adverse effects. Another important difference between PDT and PTT is the type of light sources required. Since PDT uses low fluence rates and total fluences, a variety of light-emitting diodes, relatively inexpensive low power lasers and even daylight may be used to excite photosensitizers.[19] PTT, on the other hand, requires more expensive and higher-energy lasers, complex fiber cooling and online temperature monitoring. However, the higher upfront cost of PTT equipment may be offset by the cost of photosensitizer, the need for separate appointments for photosensitized administration and longer operating room times needed for PDT irradiation.

Currently, real-time temperature monitoring for PTT is achieved through magnetic resonance (MR) thermometry, which is quite costly and requires access to an interventional MRI suite. Optical approaches, such as photoacoustic imaging[52] and diffuse optical tomography[53] have emerged as potentially more cost-effective methods of monitoring the coagulation front with higher specificity and sensitivity. Moreover, a variety of ratiometric and lifetime-based nano- and molecular thermometers are being actively investigated.[54,55] Another technique that allows to measure temperature inside the nanoparticles is X-ray absorption spectroscopy. In a recent study, Espinosa et al. described an X-ray absorption spectroscopy-based method to precisely determine the local temperature and characterize the notable nanothermal gradients of gold-based nanoparticles upon laser photoexcitation.[56]

Another critical distinguishing factor between PDT and PTT is their oxygen requirement. Effective PDT requires functional vasculature and the presence of oxygen for ROS generation, while PTT is largely oxygen-independent, which makes it suitable for treating hypoxic tumors. However, the efficacy of PTT can be limited by inadequate tumor vasculature if exogenous photoabsorbers are used to enhance heat generation. In the subsequent sections, we will discuss the various layers of PDT and PTT interplay and how the differences between these modalities can be harnessed in combination treatments.

PDT AND PTT BIOLOGICAL INTERPLAY

Both PDT and PTT have the potential to achieve localized tumor destruction safely and effectively in suitable patient cohorts, but each has specific limitations that should be considered. Thus, PDT with conventional oxygen-dependent photosensitizers is fundamentally constrained by tumor hypoxia, while PTT efficacy is limited in many cases due to the lack of heat confinement and risk of off-target damage. Combining PDT and PTT, either simultaneously or sequentially, could then harness the advantages of each modality and negate their limitations. Here, we summarized the various molecular, cellular, vascular and extravascular mechanisms that make combined PDT and PTT additive or synergistic.

Cell Death Mechanisms. Both PDT and PTT can be used to induce cytotoxicity *in vitro* and *in vivo*, but the mechanisms of

https://doi.org/10.1021/acsnano.3c00891
ACS Nano 2023, 17, 7979−8003

cell killing differ between them. PDT-induced cytotoxicity is mainly driven by the short-lived ROS, so that the photosensitizer chemical structure, subcellular localization and light delivery parameters determine dominant cell death mechanisms.[57,58] It is generally accepted that mitochondria- and endoplasmic reticulum-localizing photosensitizers trigger apoptosis *via* cytochrome C release,[59,60] while lysosomal photosensitizers induce protease release.[61] Interestingly, sequential targeting of lysosomes and mitochondria significantly enhances PDT efficacy, which could be explained by the enhanced radical formation in mitochondria as a result of photochemically triggered release of iron from lysosomes.[62] This mechanism has been leveraged in the design of a liposomal photosensitizer formulation that simultaneously targets lysosomes, mitochondria and endoplasmic reticulum.[63] Another PDT cytotoxicity mechanism involves photodamage to the antiapoptotic protein Bcl-2 that activates downstream pro-apoptotic cascade.[64] In addition to apoptosis and necrosis, PDT can also elicit autophagy and paraptosis.[65] Lastly, certain photosensitizers can induce immunogenic cell death (ICD), characterized by externalization of calreticulin (CRT) and release of adenosine triphosphate (ATP), heat shock proteins (HSP70 and HSP90) and high mobility group box 1 protein (HMGB1).[66−69]

PTT can also operate through a variety of cell death pathways, depending on temperature profile and duration, and the use of external photoabsorbers such as nanoparticles. Since heat-induced protein denaturation is the central mechanism of PTT cytotoxicity, the higher the temperature, the faster and more effective is the cell killing. Mild hyperthermia (~41−43 °C) is known to trigger HSP response but is sublethal unless maintained for an extended time (~1 h).[70−72] Coagulative PTT (55−60 °C) is thought to induce apoptosis, followed by secondary necrosis.[38] For example, gold nanoparticle-enabled PTT has been shown to induce Bid activation, leading to Bak and Bax oligomerization, triggering cytochrome c release and mitochondrial apoptosis pathway.[73,74] Another study demonstrated temperature-dependent cell death patterns in melanoma cells treated with gold nanorods.[75] Mild heating (43 °C) resulted in a relatively small loss of cell viability with 10.2%, 18.3% and 17.6% of cells undergoing apoptosis, necroptosis and necrosis, respectively. Moderate temperature increase to 46 or 49 °C increased the percentage of cells undergoing necroptosis (35.1%) and necrosis (52.8%).[75] Temperatures above the coagulative threshold (~55−60 °C) typically lead to immediate tissue necrosis due to protein denaturation and loss of cell membrane integrity. These tissue changes can be visualized with MRI,[76,77] ultrasound[78,79] or optical methods[53,80] in real time, which is advantageous for treatment monitoring and optimization.[81,82] Given the versatility of PDT and PTT cell death pathways, there are numerous ways in which they can interact.

There is a wealth of literature demonstrating that the combination of PDT with PTT or mild hyperthermia synergistically enhances tumor cell killing.[83−90] A study by Christensen and coauthors described the synergistic relationship between mild hyperthermia and PDT *in vitro*.[83] Water bath heating to 41, 42.5 and 45 °C increased cell sensitivity to PDT-induced cell death. Interestingly, this effect was sequence-dependent, with the most pronounced sensitization achieved when heating occurred between up to 1 h after the end of PDT. This suggested that hyperthermia may interfere with cell repair mechanisms that occur shortly after PDT.[83] Henderson and coauthors further investigated the sequence effects of PDT and hyperthermia combined treatment in a radiation-induced fibrosarcoma mouse model[91] and confirmed that mild hyperthermia can enhance PDT-induced cell killing when applied shortly after PDT. Finally, Chen et al. presented *in vitro*[70] and *in vivo*[88] evidence that hyperthermia administered immediately after PDT synergistically enhances cell death and tumor growth control by exacerbating cancer cell necrosis and tumor vascular damage.

The mechanisms behind the PDT/PTT synergy can be discussed on the cellular and tissue levels. In the latter, PTT can be used to target hypoxic tumor regions that can be resistant to traditional oxygen-dependent PDT. PTT may also induce additional cell death when the local oxygen levels have been depleted post-PDT. Moreover, PTT cytotoxicity can be further enhanced due to tumor acidification in poorly oxygenated tumor regions resulting from the Warburg effect.[92] Another important consideration is the dependence of PDT and PTT on the intratumoral distribution of external photoabsorbers, including nanoparticles. Tumor nanoparticle delivery is a function of tumor vascularization and avascular tumor areas are more likely to accumulate lower nanoparticle concentrations than the hypervascularized periphery. Thus, PTT using endogenous photoabsorbers may provide more even intratumoral heating and more consistent tissue photocoagulation than nanoparticle-enabled PTT regiments. Furthermore, unlike PDT, which requires photosensitizer internalization, PTT is less sensitive to the photoabsorber intratumoral distribution, as long as the target temperatures are achieved within the volume of interest. Moreover, the PTT efficacy may be further enhanced in avascular regions due to the decreased heat-sink effect and improved light tissue penetration arising from lower blood absorption.

On the cellular level, a local temperature increase has been shown to sensitize cells to PDT.[91,93] One of the contributing mechanisms is denaturation of proteins involved in DNA repair, which decreases recovery from sublethal damage.[94] This phenomenon is heavily exploited in hyperthermia-chemotherapy combination treatments;[95,96] and may be significant also in PDT-induced DNA damage. Additionally, hyperthermia has been shown to increase mitochondrial ROS levels and decrease ATP-binding cassette transporter ABCG2 efflux pump expression, leading to a decreased photosensitizer efflux and enhanced PDT efficacy.[97] The same study demonstrated that mild hyperthermia upregulates expression of heme carrier protein 1 (HCP-1) that is involved in intracellular trafficking of porphyrin photosensitizers. The upregulated HCP-1 expression, together with the downregulated ABCG2 efflux pump expression, led to the increased hematoporphyrin derivative accumulation and entrapment, thereby enhancing the PDT efficacy in a rat gastric mucosa tumor cell line, but not in normal gastric mucosa cells. Conversely, PDT can enhance cancer cell sensitivity to heat through several mechanisms. For example, tetrapyrrole-based photosensitizers have the ability to interact with the ATP-binding pocket of HSP90.[98] The direct inhibition of heat shock proteins prevents them from conducting the chaperon function and binding other important intermediates, including HIF-1α, increasing susceptibility to heat damage.[98,99] Moreover, ROS generated during PDT can directly attack heat-shock proteins, decreasing their ability to protect cancer cells against PTT.[100]

Overall, there are multiple layers of evidence suggesting that various combinations of PDT, PTT and Hx can be synergistic on both the cellular and tumor tissue levels. The mechanisms depend on the treatment sequence, temperature regimen and

https://doi.org/10.1021/acsnano.3c00891
ACS Nano 2023, 17, 7979−8003

photosensitizer structure in complex ways, so that it is necessary to determine the optimal conditions experimentally.

Vascular Effects. Both PDT and PTT exhibit dose-dependent vascular effects that can be leveraged during combination treatment. Treatment parameters, such as light fluence and fluence rate, sequencing and the interval between treatments, can significantly modulate vascular outcomes.[101] For example, mild heating increases tumor blood flow and improves hemoglobin (Hb) oxygen saturation within the tumor vasculature.[101,102] Hence, mild hyperthermia enhances tissue oxygen saturation, which can be beneficial for subsequent oxygen-dependent PDT. Tumor heating beyond Hx typically leads to a transient increase in tumor perfusion and oxygenation, followed by vascular damage and collapse. This results in a decreased tumor perfusion and oxygenation, ultimately causing necrosis. Gu and coauthors observed power density-dependent vascular effects of photothermal laser irradiation in rat breast tumor vasculature using noninvasive near-infrared spectroscopy.[103] DMBA4 tumors were irradiated with a 805 nm diode laser at power densities ranging from 0.32 to 1.27 W/cm^2 for 10 min. Tumor irradiation at 0.32 to 0.96 W/cm^2 increased intratumoral oxyhemoglobin (HbO_2) and total Hb, indicating enhanced tumor perfusion and oxygenation. However, power densities beyond 1.27 W/cm^2 and the corresponding prolonged heating beyond 55 °C reduced the total Hb concentration, indicating vascular collapse. Overall, Hx or mild and short PTT heating regimens improve tumor perfusion and oxygenation, at least in the short term, while harsher and/or prolonged heating induces vascular collapse and compromises tumor perfusion.

Given PDT's reliance on tumor oxygenation status, PTT and hyperthermia-induced vascular effects can be leveraged in a combination treatment.[91] Hx[104] and PTT[105] are known to increase tumor vascular permeability and enlarge the size of vascular pores, enabling extravasation of systemically circulating agents. This can be leveraged to enhance tumor photosensitizer accumulation and boost PDT efficacy. However, PTT regimens that cause vascular damage and decreased blood flow may compromise the effectiveness of subsequent oxygen-dependent PDT.

Like PTT, PDT is also known to cause a variety of vascular effects, including vasoconstriction/vasodilation,[106,107] changes in vascular permeability[13] and vascular collapse.[108−110] Several studies demonstrated that PTT and mild hyperthermia may exacerbate PDT-induced vascular damage, leading to tumor starvation. Kimel et al. investigated the effects of tetraphenylporphine tetrasulfonate-PDT combined with hyperthermia (48 °C) on vascular damage in a chick chorioallantoic membrane (CAM) model.[111] Combining PDT with hyperthermia increased the damage score in the CAM vasculature by ∼40%. Another study by Kelleher and coauthors investigated the effects of mild hyperthermia (43 °C) in combination with bacteriochlorophyll serine-based PDT in rats bearing DS-sarcomas.[112] The combined treatment led to a marked decrease in tumor perfusion and oxygenation, leading to a switch from oxidative to glycolytic metabolic state. In addition to causing direct vascular damage, PDT changes vascular permeability, which has significant implications for the delivery of systemic agents. It has been shown that subtherapeutic PDT doses can increase tumor perfusion, cause vasodilation and enhance vascular leakiness toward macromolecular agents.[9,110] In the context of combination with PTT, this can be leveraged to promote the accumulation of photoabsorbing nanoparticles and boost treatment efficacy. Therapeutic PDT doses, however, cause thrombocyte activation and vascular occlusion, which would compromise tumor perfusion and the subsequent delivery of systemic agents.

Overall, both PDT and PTT have pronounced dose-dependent vascular effects that profoundly influence the tumor microenvironment and efficacy of other therapies. Hence, in designing PDT/PTT combination treatments, the following points should be considered. First, successful PDT requires noncompromised tumor perfusion. Conducting coagulative PTT prior to PDT would induce vascular collapse, decrease tumor oxygenation and PDT efficacy. Subcoagulative PTT doses and or mild hyperthermia can increase tumor oxygenation and thereby enhance the efficacy of subsequent PDT. PTT, on the other hand, is less dependent on tumor oxygenation. Furthermore, hypoxia and tumor acidification that occur after PDT can sensitize cells to PTT, while decreased tumor blood flow can reduce the "heat sink" effect and help achieve photocoagulation temperatures. Therefore, conducting PTT after PDT treatment may result in synergistic effects through a variety of different mechanisms.

Extracellular Matrix Effects. Both PDT and PTT have distinct effects on the extracellular matrix (ECM).[113] Their impact on the tumor-surrounding ECM has significant implications for preserving tissue architecture and healing. At the same time, intratumoral ECM modulation impacts tumor perfusion, drug delivery and treatment response. Most solid tumors are characterized by the increased ECM content, including proteins (most notably collagen, elastin and fibronectins),[114] glycoproteins, proteoglycans[115] and polysaccharides.[116,117] This aberrant ECM deposition results in increased solid tissue stress that, together with elevated interstitial tumor pressure, can collapse tumor blood vessels and compromise systemic drug delivery.[118] Furthermore, the presence of perivascular collagen sleeves impedes the diffusion of macromolecular drugs and nanoparticles, preventing them from reaching cancer cells.[119] Hence, tumor desmoplasia is an emerging therapeutic target and there is a significant interest in using PDT and PTT to overcome it.

A study conducted by Barr and coauthors examined the effects of PTT on the ECM.[120] Rat colon was treated with 675 nm laser light at 500 mW for 100 s (50 J), resulting in a local temperature increase up to 66 ± 7.5 °C. Transmission electron microscopy demonstrated significant swelling and structural changes in the submucosal collagen from thermal injury, likely caused by protein denaturation. Furthermore, these changes were absent in colon treated with hematoporphyrin derivative-PDT-treated colon (100 mW for 500 s, 50 J), indicating that PDT preserves the surrounding ECM structure. More recently, Raeesi and Chan investigated PTT effects in a collagen (I) matrix gel barrier model.[12] Tumor PTT was simulated by including gold nanoparticles in a gel and subjecting it to 785 nm NIR laser irradiation (3 W/cm^2 for 6 min), yielding temperature increase in the 45−55 °C range. This led to collagen denaturation, increased permeability and diffusivity of 50−120 nm nanoparticles by ∼14 and ∼21 times, respectively. These findings inspired a variety of tumor xenograft studies, directed at leveraging this phenomenon and improving tumor drug delivery.[121] For example, a study by Marangon et al. investigated the effects of carbon nanotube- and iron oxide nanoparticle-induced subcoagulative PTT (52 °C for 3 min) and mild hyperthermia (43 °C for 15 min) on the ECM structure and deposition, as well as tumor stiffness in subcutaneous epidermoid carcinoma tumors.[122] Shear-wave elastography

https://doi.org/10.1021/acsnano.3c00891
ACS Nano 2023, 17, 7979−8003

showed that both PTT and mild hyperthermia decreased tumor stiffness for up to 9 days post treatment, which corresponded to a delayed tumor growth compared to untreated controls. This was likely driven by the denaturation and disruption of collagen bundles, as demonstrated using Masson's Trichrome staining, transmission electron microscopy and second harmonic generation (SHG) microscopy. Overall, these results suggest that nanoparticle-assisted PTT could induce profound structural changes in a tumor ECM, including collagen reorganization, thereby enabling more effective drug tumor penetration.

Unlike PTT, PDT has long been viewed as an ECM-sparing technique.[29,120,123] The ability of PDT to specifically target cells and preserve collagen structures around lesions is extensively used in dermatology, enabling treatment of large actinic keratosis lesions, melanoma, or acne with virtually no scarring.[124] There is less known, however, about PDT effects on the intratumoral ECM. Nelson et al. described collagen fragmentation in the subendothelial zone of tumor capillaries as early as 1 h post PDT, followed by edema and vascular collapse.[125] These ultrastructural observations provided useful insights but were qualitative and not supported by histopathological analysis. Our group recently investigated the effects of subtherapeutic PSMA-targeted photodynamic treatment (50 J/cm^2) in a subcutaneous prostate tumor xenograft.[11] Subtherapeutic PDT decreased the overall tumor collagen density by ∼2-fold, as demonstrated by Masson's trichrome staining, and reduced collagen coverage within the subendothelial areas revealed by electron microscopy. We hypothesized that these changes contributed to the observed nanoparticle delivery enhancement. Another study by Obaid and colleagues reported that PDT using EGFR-targeted benzoporphyrin derivative-containing nanoconstructs decreased collagen deposition in desmoplastic pancreatic ductal adenocarcinoma (PDAC).[126] There was ∼1.5-fold decrease in collagen density compared to untreated controls. Interestingly, collagen photomodulation depended on EGFR targeting and did not occur when the photosensitizer (BPD) was delivered in nontargeted liposomes. Moreover, it has been shown that photoimmunoconjugates of BPD are significantly more phototoxic in high-collagen content spheroids compared to the classic liposomal formulation.[127] Subsequent *in vivo* studies using targeted photoactivable multi-inhibitor liposomes (TPMILs) revealed that PDT can effectively remediate desmoplasia in PDAC tumors by reducing collagen density by >90% and increasing collagen nonalignment by >10^3-fold as demonstrated by SHG microscopy.[128] Excitingly, this approach doubled the survival in PDAC-bearing mice, highlighting the important role that PDT may play in combating the effects of desmoplasia.

Overall, there is a notable difference in how PDT and PTT affect the ECM within tumors as well as in the surrounding tissues. Due to its sharp treatment boundary and nonthermal nature, PDT allows sparing of the surrounding ECM structures, facilitating healing and reducing scarring. On the other hand, PTT is associated with a higher risk of collagen damage around the tumor area. Both PDT and PTT can induce changes in the tumor ECM structure and content, which may be harnessed in drug delivery. To our knowledge, there are no studies investigating changes in tumor ECM using combined PDT/PTT treatments. Depending on the treatment regimen, we hypothesize that such changes could contribute to treatment synergy in various ways. For example, subjecting a tumor to light-induced mild hyperthermia could soften the tumor ECM, promoting extravasation and interstitial diffusion of photosensitizer. Conversely, PDT pretreatment could disrupt perivascular collagen sleeves, promoting deeper penetration of heat-generating nanoparticles. Hence, the ECM effects of PDT and PTT have potential therapeutic utility that could be harnessed in combined treatment protocols.

Immune Effects. Another important biological aspect of PDT and PTT is their ability to elicit an immune response[67,129,130] by releasing tumor-specific antigens as well as by producing adjuvant-like molecules, CRT, HSPs, HMGB1 and ATP.[131,132] Large numbers of cells undergoing ICD trigger acute inflammation, caused by the release of inflammatory cytokines (IL-1β, IL-6, TNFα and CXCL2) and tumor immune-cell infiltration. This initial inflammation promotes the activation and recruitment of dendritic cells that, by processing and presenting tumor-associated antigens, activate the adaptive arm of the immune system. Ultimately, the activation of CD4+, CD8+ and Treg cells leads to primary tumor regression and, under certain conditions, can result in the abscopal effects (destruction of separate primary and secondary metastatic tumor lesions). In addition to activating the adaptive immune response, both PDT and PTT have been shown to reprogram tumor-associated macrophages from tumor-promoting to tumor-inhibiting, which helps control tumor growth and enhances the efficacy of immunotherapies.

However, there are several key differences between the PDT- and PTT-triggered immune responses. While both PDT- and PTT-induced cell death can be immunogenic, PTT can only induce ICD in a specific thermal window. Sweeney et al. investigated ICD induction in neuroblastoma cells using Prussian blue nanoparticles.[133] They found that the expression of ICD markers, including the release ATP and HMGB1 and cell surface display of CRT, was most pronounced after the cells were heated to 50−60 °C for 10 min. Temperatures below 50 °C or above 60 °C were ineffective, suggesting that the PTT dose may be relatively more important than PDT dose in generating ICD. There are numerous studies describing the immune-stimulating potential of PDT and PTT in breast,[134] mesothelioma,[135,136] colon and lung[137] and pancreatic[138] tumor models.[130]

While certain PDT regimens, particularly repeated PDT treatments, have been shown to activate the adaptive immunity and induce abscopal effects alone,[135,136] PDT and PTT typically require additional immunoadjuvants or immune response-promoting agents. This is often achieved by using multifunctional nanoparticles that combine photoactive, chemotherapeutic and immune-stimulating agents.[139] For example, a recent study by Ghosh et al. combined irinotecan-loaded porphyrin−phospholipid liposomes with anti-programmed cell death 1 (PD-1) and anti-cytotoxic T-lymphocyte-associated protein 4 (CTLA-4) antibodies in KPC pancreatic cancer tumors.[138] Chemophototherapy and immunotherapy alone were unable to eliminate small KPC tumors. But in combination, they effectively eliminated not only small (∼100 mm^3) but also medium-sized (∼200 mm^3) KPC tumors and imparted protection against tumor rechallenge. The observed synergistic interaction between the two modalities was in part facilitated by PDT-induced enhancement of anti-PD-1 antibody tumor accumulation and penetration. In another study, Zhang et al. designed polyphenol derivative-based nanoparticles for the simultaneous chlorin e6-enabled PDT and gossypol chemotherapy.[140] PDT with the designed nanoconstruct led to the release of ATP and HMGB1, as well as the maturation of dendritic cells *in vitro*. Its combination with the PD-L1

https://doi.org/10.1021/acsnano.3c00891
ACS Nano 2023, 17, 7979−8003

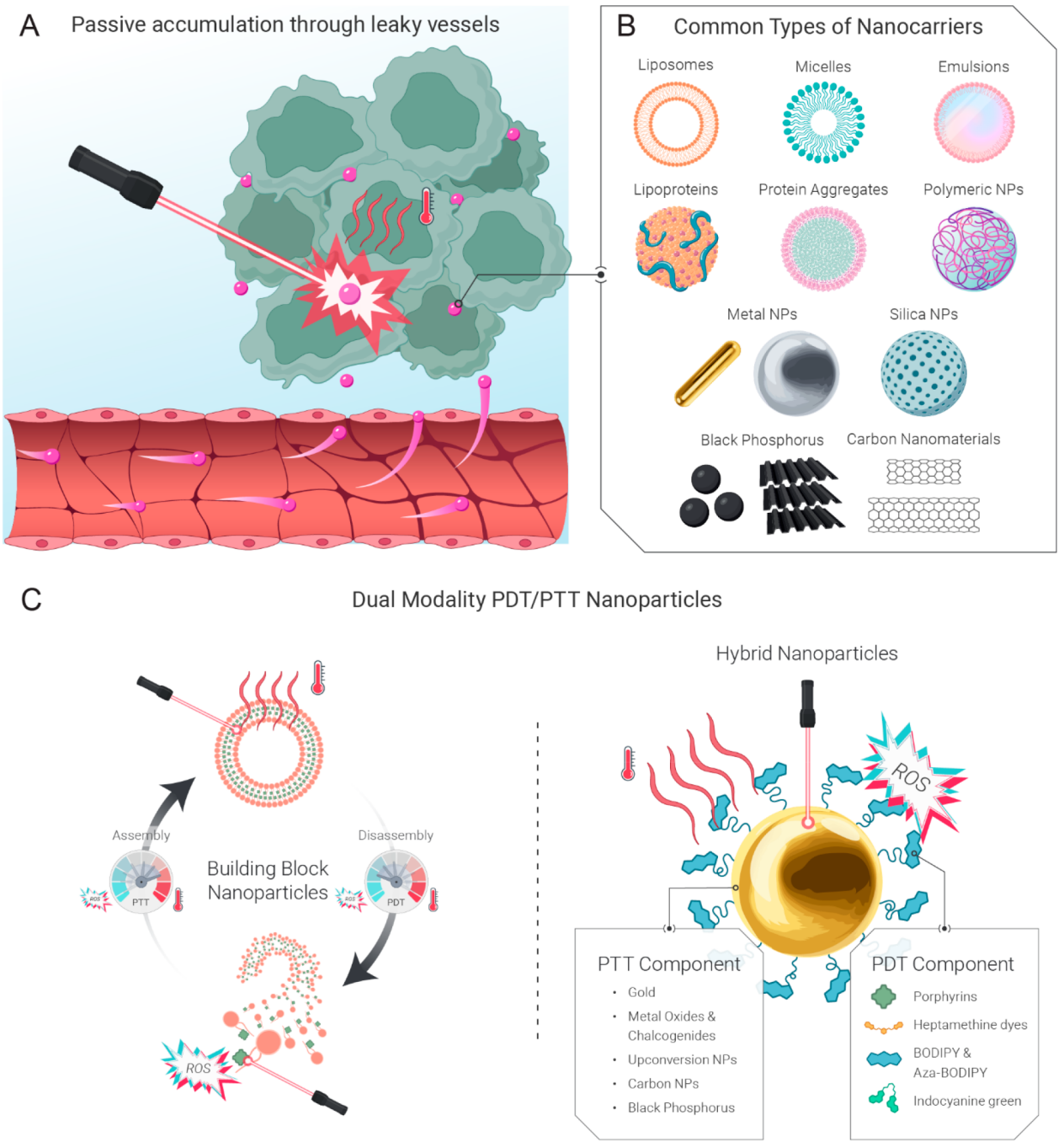

Figure 2. Use of nanoparticles for dual PDT/PTT treatment. A. Nanoparticles passively accumulate in tumors due to the EPR effect, where they can be activated with light to produce ROS or heat. B. Common delivery vehicles include liposomes, micelles, nanoemulsions, lipoproteins and lipoprotein mimetics, protein-based nanoparticles, polymeric nanoparticles, metal, silica, black-phosphorus and carbon-based nanomaterials. C. Left panel: PDT/PTT-active nanoparticles can be designed with a single monomer that can act as a PTT agent within an intact nanostructure and a PS upon dissociation. Right panel: Hybrid PDT/PTT-active nanoparticles can incorporate two or more photoactive agents, one of which acts as a PS, while another enhances heat generation.

checkpoint blockade inhibited the growth of distant tumors and metastasis in an immunocompetent 4T1 breast cancer model.

Similarly to PDT, PTT immune-stimulating effects can be enhanced by immunotherapies. For example, combining black phosphorus nanosheets-enabled PTT with anti-CD47 antibodies improved the treatment's effectiveness and led to the abscopal effects in the A20 subcutaneous B-cell lymphoma model in BALB/c mice.[141] Intratumoral injection of the nanosheets combined with 808 nm laser irradiation (1.0 W/cm^2, 10 min) led to a local temperature increase up to ~51 °C. When black phosphorus-enabled PTT was combined with anti-CD47 antibodies, it caused tumor-associated macrophages to shift from a tumor-promoting M2 to a tumor-suppressing M1 phenotype. The anti-CD47 antibodies abrogated the CD47/SIRPα interaction, which helped promote phagocytosis and facilitated presentation of the tumor-associated antigens. This led to the activation of tumor-specific T-cells and inhibition of distant tumors through abscopal effects.

https://doi.org/10.1021/acsnano.3c00891
ACS Nano 2023, 17, 7979−8003

Table 2. Summary of Recently Published Dual PDT/PTT Agents Utilizing a Single Photoactive Component

Photoactive Agent	NP Type	Description	Photothermal Conversion Efficiency (η)	Tumor Model	Treatment Parameters	Ref
Porphyrin	Liposome-like nanoparticles	~100 nm porphyrin-lipid liposomes, PTT-active while intact, PDT-active when disrupted	–	KB SQ model of hypoxia (PTT)/hyperoxia (PDT), IV injection	PDT: 671 nm laser (222 mW/cm^2, 318 s); PTT: 671 nm laser (833 mW/cm^2, 85 s)	167, 169, 173
	Pyropheophorbide a/doxorubicin/PEG nanoporphyrins	~20 nm assemblies, PTT-active while intact, PDT-active when disrupted	–	SKOV3 SQ and transgenic mammary cancer mouse model, IV injection	PDT/PTT: 690 nm diode system (1.25 W/cm^2, 2 min)	185
	Porphyrin-peptide nanodots	~20 nm assemblies, PTT-active while intact	54.2%	MCF-7 SQ model, IV injection	PDT: Not tested; PTT: 635 nm laser (0.3 W, 10 min)	186
	Tetra (p-amino-phenyl) porphyrin covalent organic frameworks	Low quenching, simultaneously PDT- and PTT-active	15.0%	4T1 SQ tumor model, IT injection	PDT/PTT: 635 nm laser (1.5 W/cm^2, 5 min)	187
	Pheophorbide a- hydrazone-doxorubicin multimicelle aggregates	Size-transformable, pH-sensitive	–	OSC-3 SQ and orthotopic oral cancer model; IV injection	PDT/PTT performed in three cycles once per week (680 nm laser, 3 min, 0.4 W/cm^2)	188
ICG	Hyaluronan and folate-targeted ICG	Negatively charged NPs (~130 nm) consist of 30 nm positively charged NPs (<30 nm) coated by folic acid- and dopamine-decorated hyaluronan	–	B16 SQ melanoma model, IV injection	PDT: 808 nm laser (1 W/cm^2, 60 s, no temperature elevation noted)	189
	Mesoporous calcium silicate	TAM-targeting (HA, Man); pH responsive	30.3%	4T1 SQ tumor model, IV injection	PDT/PTT: 808 nm laser (2.0 W/cm^2, 3 min, 51.8 °C)	190
	Human serum albumin (HSA)- ICG aggregates	~75 nm HSA-ICG nanoparticles, PDT/PTT-active, fluorescence/photoacoustic image guidance	–	4T1 orthotopic model, IV injection	PDT: 808 nm laser (0.8 W/cm^2 for 5 min, interrupted irradiation (5 min break after each min of light) to avoid temperature increase); PDT/PTT: 808 nm laser (0.8 W/cm^2 for 5 min, 57.2 °C)	175
Heptamethine-based dyes	IR-780-loaded transferrin-based nanoplatform	>100 nm, long plasma circulation time (~20 h), transferrin receptor targeting	–	CT26 SQ tumor model, IV injection	PDT/PTT: 808 nm laser (1 W/cm^2, 5 min, ~50 °C)	191
	HA-stabilized fluorocarbon-IR-780 assemblies	Fluorocarbon-based IR-780 NPs, both PDT and PTT active at the same time.	25.4%	4T1 tumor model, IV injection	PDT/PTT: 808 nm laser (2.2 W/cm^2, 5 min)	192
BODIPY and Aza-BODIPY	pH-sensitive BDP-Oxide NPs self-assembled with PEG-b-PDPA	pH-dependent fluorescence and PDT activation; under hypoxia CYP450-mediated reduction switches it to PTT/photoacoustic	BDP – 40.2%, BDP-oxide – 12.6%	HepG2 SQ tumor model, IV injection	PDT/PTT: 730 nm laser (0.3 W/cm^2, 5 min)	166
	DSPE-PEG2000-BODIPY nanoparticles	BODIPY-based nanoparticles with tunable absorption wavelength	60.5%	HeLa tumor model, IV injection	PDT/PTT: 660, 730, or 808 nm laser (1 W/cm^2, 8 min, 40–55 °C)	193
	Polymeric BODIPY vesicles	Wavelength-dependent polymeric BODIPY vesicles, PDT-active at 660 nm, PTT-active at 785 nm	16.0% - 29.0%	4T1 tumor model, IV injection	PDT: 660 nm laser (0.5 W/cm^2, 300 s); PTT: 785 nm laser (0.5 W/cm^2, 300 s)	194
Black phosphorus (BP)	BP nanosheets	BP nanosheet-based drug delivery system for synergistic PDT/PTT/chemotherapy	–	4T1 SQ tumor model, IT injection	PDT: 660 nm laser (0.5 W/cm^2, 15 min); PTT: 808 nm laser (1 W/cm^2, 5 min, 53.7 °C)	195

https://doi.org/10.1021/acsnano.3c00891
ACS Nano 2023, 17, 7979–8003

While most studies focus on the immune-stimulating effects of PDT and PTT, the unregulated inflammatory response may result in permanent tissue injury, undermining phototherapy-triggered immunogenicity and even promote tumor regrowth. To strike a balance between pathological and protective immune responses, a recent study by Li et al. explored an H_2S gas-based strategy, which utilized an amphiphilic-conjugated polymer with a polysulfide-based hydrogen sulfide (H_2S) donor.[142] The polysulfide donor released H_2S upon the exposure to intracellular glutathione, leading to mitochondrial dysfunction and a strong anti-inflammatory effect. This gas-modulated PTT strategy inhibited tumor growth in a 4T1 breast cancer mouse model and limited the release of proinflammatory cytokines, such as tumor necrosis factor-alpha (TNF-α), interleukin-6 (IL-6) and interleukin-1beta (IL-1β). Moreover, the regulated inflammation accelerates PTT-induced wound healing.

Most studies focus on the interaction between either PDT or PTT with immunotherapies, but it remains unclear how PDT and PTT interact with one another in the context of immune stimulation. Evidence suggests that hyperthermia can facilitate tumor immune cell infiltration, which could boost PDT-induced immunity.[143−145] Sublethal temperatures (<50 °C) induce heat shock proteins that can complement PDT-induced cytokine release and exacerbate inflammation. Despite significant preclinical progress, PDT and PTT immune stimulation are yet to be harnessed clinically to their full potential. Recently, a phase 2 clinical trial was launched of the combination of PDT with anti-PD1 checkpoint inhibitor in pleural mesothelioma patients (identifier NCT04400539). The ability of PTT to interact with immunotherapies, however, is yet to be investigated in the clinic.

DUAL MODALITY PDT/PTT NANOPARTICLES

Significant advances have been made in developing multifunctional nanomaterials suitable for both PDT and PTT.[146] Nanoparticles between 10 and 200 nm have the propensity to selectively accumulate in tumors due to the enhanced permeability and retention (EPR) effect (Figure 2A).[147,148] Hence, the use of photoactive nanoparticles not only increases tissue heating and enables ROS generation but also imparts an additional level of selectivity to PDT and/or PTT. In the case of PDT, PS incorporation into a nanoparticle often leads to fluorescence and ROS quenching, which is restored upon its dissociation at the tumor site. This phenomenon can help minimize unwanted photosensitivity and off-target effects and achieve high-payload PS delivery.[149−151] The use of nanoparticles as external photoabsorbers for PTT helps decrease the amount of external energy needed to achieve photothermal effect and facilitates tissue sparing as long as they possess a certain degree of tumor selectivity. The tumor-to-tissue ratio can be further enhanced by tuning the nanoparticle size, shape and surface chemistry or by incorporating targeting ligands.[152]

Various organic and inorganic nanoparticles are being explored as vehicles for the delivery of photoactive agents (Figure 2B,C).[153,154] Liposomes, micelles, nanoemulsions, protein- and polymer-based nanoparticles offer excellent biocompatibility, are easily degradable and can be loaded with a variety of PDT and/or PTT active molecules. Inorganic materials, including gold and metal oxide nanoparticles, silica, upconversion nanoparticles and quantum dots are characterized by high photothermal conversion coefficients and can be functionalized with photosensitizers.[24,153] For example, gold nanoparticles, including nanoshells, nanostars, nanorods and nanospheres have attracted significant interest in the field of PTT due to their high photothermal conversion coefficients, synthetic tunability and favorable safety profiles.[155] Carbon- and more recently black phosphorus-based materials represent yet another nanoparticle class with interesting photophysical properties.[156,157] Black phosphorus nanodots and nanosheets are being actively investigated as PDT and PTT agents due to their intrinsic absorption and ROS-generating properties.[158158−160] For a more comprehensive overview of these and related nanomaterials the reader is encouraged to refer to several recent review articles.[148,149,151,161,162]

Among the wide variety of nanomaterial classes and formulations, two primary design approaches can be distinguished, with one relying on a solitary PDT/PTT active monomer, and the other incorporating two or more photoactive materials within a single nanoparticle construct. In the former approach, nanoparticles contain a photoactive monomer capable of functioning as both a PDT and PTT agent.[163] The most common monomers of interest are organic dyes, such as porphyrins,[164] ICG, heptamethine and BODIPY-family dyes (Table 2). These and other photoactive molecules can be integrated into liposomal, lipoprotein, micelle-like, peptide-based or polymeric nanostructures, which modifies their pharmacokinetics and biodistribution and enables high payload delivery of photoactive agents. This approach minimizes the number of nanoparticle components, streamlining manufacturing and scale-up.[165] From the photophysical perspective, incorporating a monomer into nanoparticles often leads to aggregation-induced quenching of fluorescence and ROS generation, with the light energy being dissipated as heat.[149−151] It is then common that these nanoparticles act as PTT agents while intact and as PDT agents once dissociated upon cellular uptake. This phenomenon can be utilized to design activatable PDT agents that can minimize the off-target effects and photosensitivity. Within this paradigm, a nanoparticle is thought to remain largely inactive until it reaches the tumor and binds a receptor or dissociates within the acidic environment. One of the consequences is that the optimal time points for PDT and PTT are likely to be different. However, it could be possible to find a time point during which nanoparticle's intact and disrupted states are at an optimal ratio that enables both therapies simultaneously. Another important consideration in such design is whether the monomer's supramolecular interactions within the nanostructure change its absorption spectrum. Nanostructure-induced spectral changes may then require two separate light sources with the appropriate wavelengths for PDT and PTT.[166]

A prime example of this approach is porphysomes that are liposome-like nanoparticle containing a large (~80 000) number of porphyrin-lipid building blocks (Figure 3A).[167] This high porphyrin packing density leads to >99% quenching of fluorescence and ROS generation, making intact porphysomes potent photothermal agents, as demonstrated in several preclinical studies (Figure 3B,C).[167,168] When porphysomes are disrupted, the porphyrin's fluorescence and photodynamic activity are recovered, enabling PDT[169] and fluorescence image guidance.[170−172] By adding surface targeting ligands, such as folate, the dissociation kinetics can be shifted toward rapid activation, making them more suitable for PDT.[173] Importantly, recent evidence suggests that the original nontargeted porphysomes exhibit similar PDT efficacy as a clinical photosensitizer Photofrin (Figure 3D),[169] indicating that porphysomes can be used as dual PDT/PTT agents with the

https://doi.org/10.1021/acsnano.3c00891
ACS Nano 2023, 17, 7979−8003

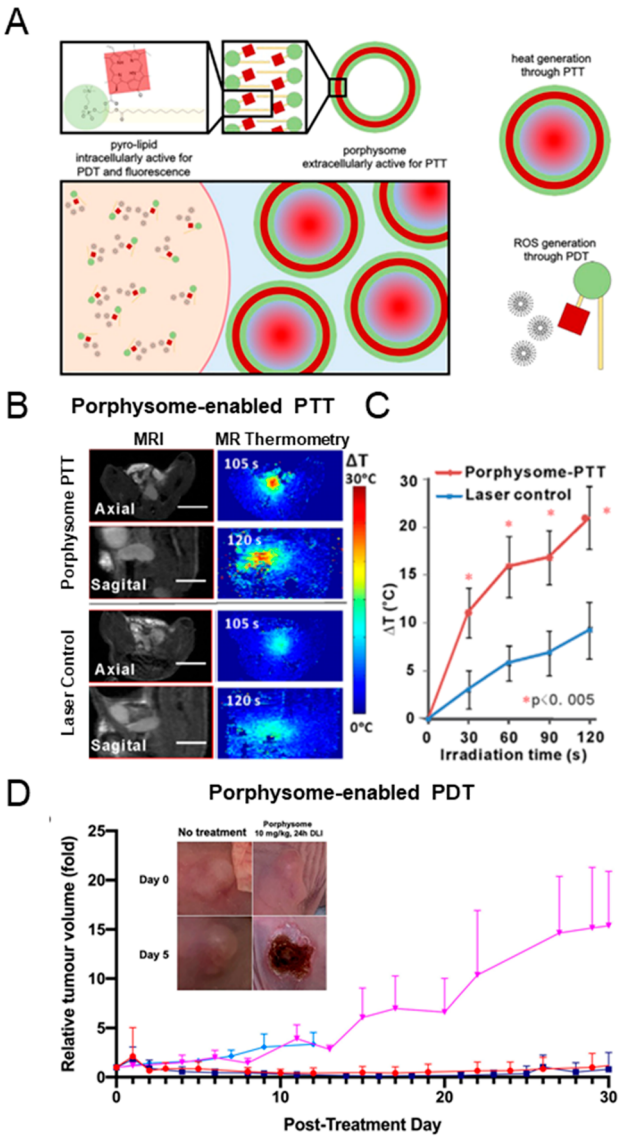

Figure 3. Porphysome nanovesicles as a dual PDT/PTT agent. A. Schematic representation of the structure and function of porphysomes and the porphyrin-lipid (pyro-lipid) building blocks. Intact porphysomes in the extracellular space remain fluorescently and photodynamically quenched and have the capacity to generate heat upon 671 nm laser irradiation (lower panel, right). When are dissociated upon cellular uptake, the ROS generation is unquenched, resulting in PDT activity (lower panel, left). Adapted with permission under a Creative Commons Attribution 4.0 International (CC BY 4.0) License from ref 169. Copyright 2021 Keegan Guidolin et al., published by De Gruyter. B. Porphysome-enabled PTT in an orthotopic prostate tumor model. *In vivo* MR-thermometry demonstrates a significant temperature increase in animals injected with porphysomes upon laser irradiation. Left panel: MRI images of orthotopic prostate tumors from axial and sagital directions. Right panel: MR-thermometry map. C. Quantification of temperature increase in a prostate tumor during the laser irradiation process (mean ± SD, n = 5). Adapted with permission from ref 174. Copyright 2016 Wiley Periodicals, Inc. D. Relative tumor volume change in animals bearing subcutaneous A549 lung tumors treated with porphysome-PDT (red), Photofrin-PDT (dark blue), porphysomes-only (magenta) and Photofrin-only (light blue) up to 30 days post PDT (mean ± SD, n = 5). Adapted with permission under a Creative Commons Attribution 4.0 International (CC BY 4.0) License from ref 169. Copyright 2021 Keegan Guidolin et al., published by De Gruyter.

same 671 nm laser, thereby simplifying treatment logistics and offering the therapeutic benefits of the combined PDT/PTT treatment.

Another example of a dual PDT/PTT nanoparticle that utilizes a single photoactive agent is human serum albumin-ICG conjugates (Figure 4A).[175] Sheng and coauthors designed human serum albumin (HSA)-indocyanine green (ICG) (HSA-ICG) nanoparticles by intermolecular disulfide conjugation. This simple 2-component platform demonstrated favorable pharmacokinetics and biodistribution, resulting in a tumor-to-normal tissue ratio of 36.12 ± 5.12 at 24 h post intravenous injection (Figure 4B). Given the light-absorbing and PDT properties of ICG, the authors tested the PDT/PTT efficacy in subcutaneous and orthotopic 4T1 breast cancer tumor models under a single-wavelength NIR laser irradiation (Figure 4C,D). Treatment (808 nm, 0.8 W/cm^2 for 5 min, ~57 °C) effectively suppressed tumor growth for up to 40 days. To ascertain the contribution of PDT to this observed response, one cohort of HSA-ICG-injected mice received interval laser irradiation, which prevented temperature increase: irradiation was stopped every minute and the tumor was allowed to cool down for 5 min. While the total light dose remained the same, the tumor temperature did not exceed 32.4 °C. This regimen resulted in moderate control over tumor growth, inferior to the dual PDT/PTT treatment. One of the limitations of this study was the lack of a PTT-only group, which would enable quantification of the interaction between PDT and PTT and establish synergy. Overall, this protein-based system produced a robust *in vivo* tumor response and warrants further investigation.

While in most cases incorporating a photoactive agent into a nanoparticle leads to aggregation-induced quenching, in some cases it can facilitate different photophysical phenomena, including ordered aggregation.[150,176] For example, it has been demonstrated that the incorporation of bacteriochlorophyll-lipid within liposomal[177−179] or lipoprotein mimetic[180,181] nanoplatforms can lead to J-aggregation characterized by a red shift in the absorption spectrum. Having two distinct spectral signatures that correspond to the alternate nanoparticle states (750 nm absorption peak for monomers, 820 nm for the intact nanoparticles) can be used to obtain structural nanoparticle information *in vitro* or *in vivo*. Additionally, these distinct spectral characteristics may be harnessed for dual-wavelength PDT/PTT, wherein the longer-wavelength 820 nm light is absorbed by the nanoparticles in the intact state, while 750 nm light can excite the monomers for subsequent PDT. Interestingly, J-aggregation is intrinsically a temperature-dependent phenomenon, but local temperature increase during PTT treatment can disrupt J-aggregates and serve as an internal on/off-switch.[182] This may be leveraged to gradually decrease light attenuation as the target temperature is reached, resulting in increased light transmission and heating depth.

Another important factor that determines a photoabsorber's PDT/PTT properties within a nanoparticle is its lipid environment. A recent study by our group demonstrated that the nature of a lipid conjugate determines porphyrin quenching stability within a lipoprotein nanoparticle.[183] For example, the incorporation of a porphyrin moiety as an oleylamide conjugate yields highly quenched nanoparticles with low fluorescence and

https://doi.org/10.1021/acsnano.3c00891
ACS Nano 2023, 17, 7979−8003

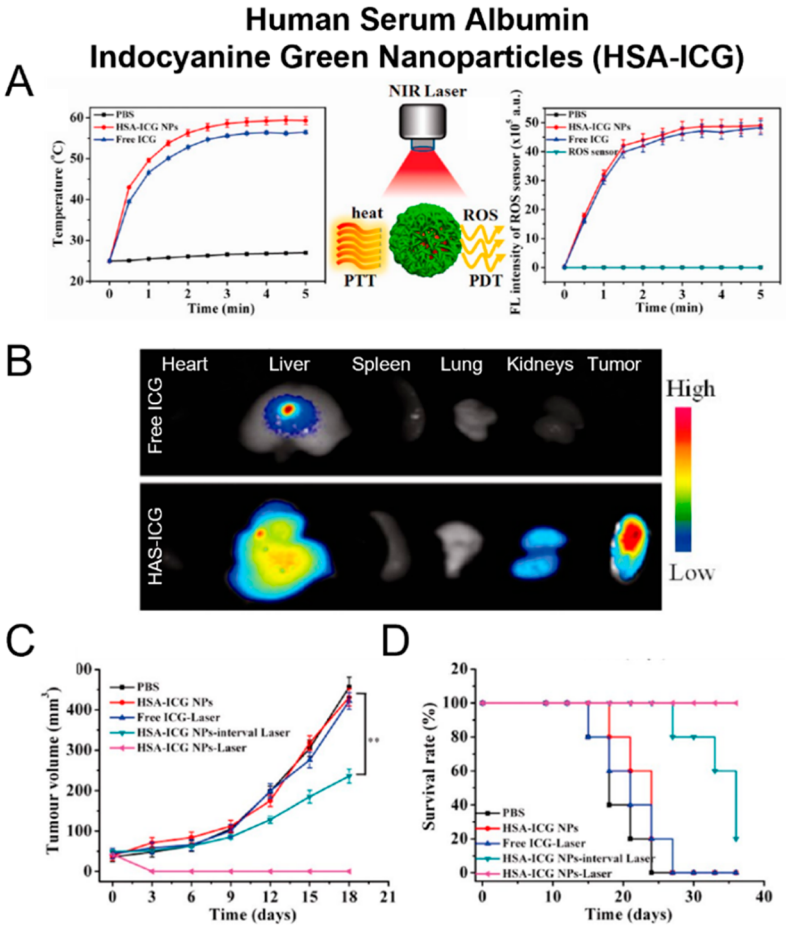

Figure 4. Human serum albumin-ICG (HSA-ICG) nanoparticles as a single-agent PDT/PDT nanoplatform. A. Time-dependent heat (left) and singlet oxygen generation (right) during NIR laser irradiation. B. *Ex vivo* fluorescence biodistribution of free ICG and HSA-ICG nanoparticles 24 h post IV injection. C. Tumor growth curves and D. survival rates of mice bearing orthotopic 4T1 tumors after different treatments. PDT only: HSA-ICG NPs-interval laser; PDT + PTT: HAS-ICG NPs-laser. (n = 5, $^{**}p < 0.01$). Adapted with permission from ref 175. Copyright 2014 American Chemical Society.

PDT activity but strong photoacoustic signal *in vivo*. Porphyrins conjugated to an amphiphilic lipid moiety showed weaker quenching and stronger ROS generation within a nanoparticle. We hypothesize that the hydrophobicity of a lipid conjugate affects its dissociation kinetics *in vivo*, which can be leveraged in the design of primarily PDT- or PTT-active agents. Another study demonstrated that incorporating a porphyrin-lipid conjugate into liposomes formed of saturated or unsaturated lipids switches the dominant de-excitation route of J-aggregates by promoting primarily heat or ROS generation, respectively.[179] Therefore, by changing the lipid environment within a nanoparticle one can tune its photophysical properties.

As discussed above, nanoparticles exhibiting aggregation-induced-quenching often suffer from a low singlet oxygen quantum yield, making it challenging to conduct PDT and PTT simultaneously. Furthermore, upon nanoparticle dissociation, monomers become more susceptible to photobleaching. To address this challenge, Zhao and colleagues designed a discretely integrated nanofabrication (DIN) platform that combined cisplatin, ICG and a polymeric spacer (PES) (Figure 5).[184] By optimizing the ICG/polymer stoichiometry, aggregation-induced quenching, photobleaching and photosensitizing properties could be balanced, yielding an agent that could simultaneously perform PDT, PTT and chemotherapy (Figure 5A,B,C,D). Importantly, triple PDT/PTT/chemotherapy treatment triggered the release of danger-associated molecular patterns and facilitated the downstream immune activation events, including dendritic cell maturation, activation of cytotoxic T lymphocytes, cytokine release and macrophage repolarization. As a result of this robust immune activation, DIN-enabled phototherapy not only suppressed primary tumor growth but also delayed the progression of a distant nodule (Figure 5E,F,G).

An alternative approach to the design of the dual PDT/PTT nanoparticles integrates two or more types of materials within a single nanoparticle, one of which imparts photosensitization while the other offers high photothermal conversion efficiency (η). Inorganic materials such as gold,[155,196,197] iron oxide, quantum dots, rare earth-doped nanocrystals, carbon-based nanoparticles or hollow silica[198] can be combined with various photosensitizing agents and their surface can be further functionalized to improve pharmacokinetics or impart targeting.[199] Gold nanostructures are the most studied class of plasmonic nanomaterials for PTT. Due to their high photothermal conversion efficiency, synthetic tunability, inertness and biocompatibility, they are excellent candidates for PDT/PTT agent design.[155] Finally, more advanced approaches are being developed, wherein the nanoparticle PDT/PTT properties are

https://doi.org/10.1021/acsnano.3c00891
ACS Nano 2023, 17, 7979−8003

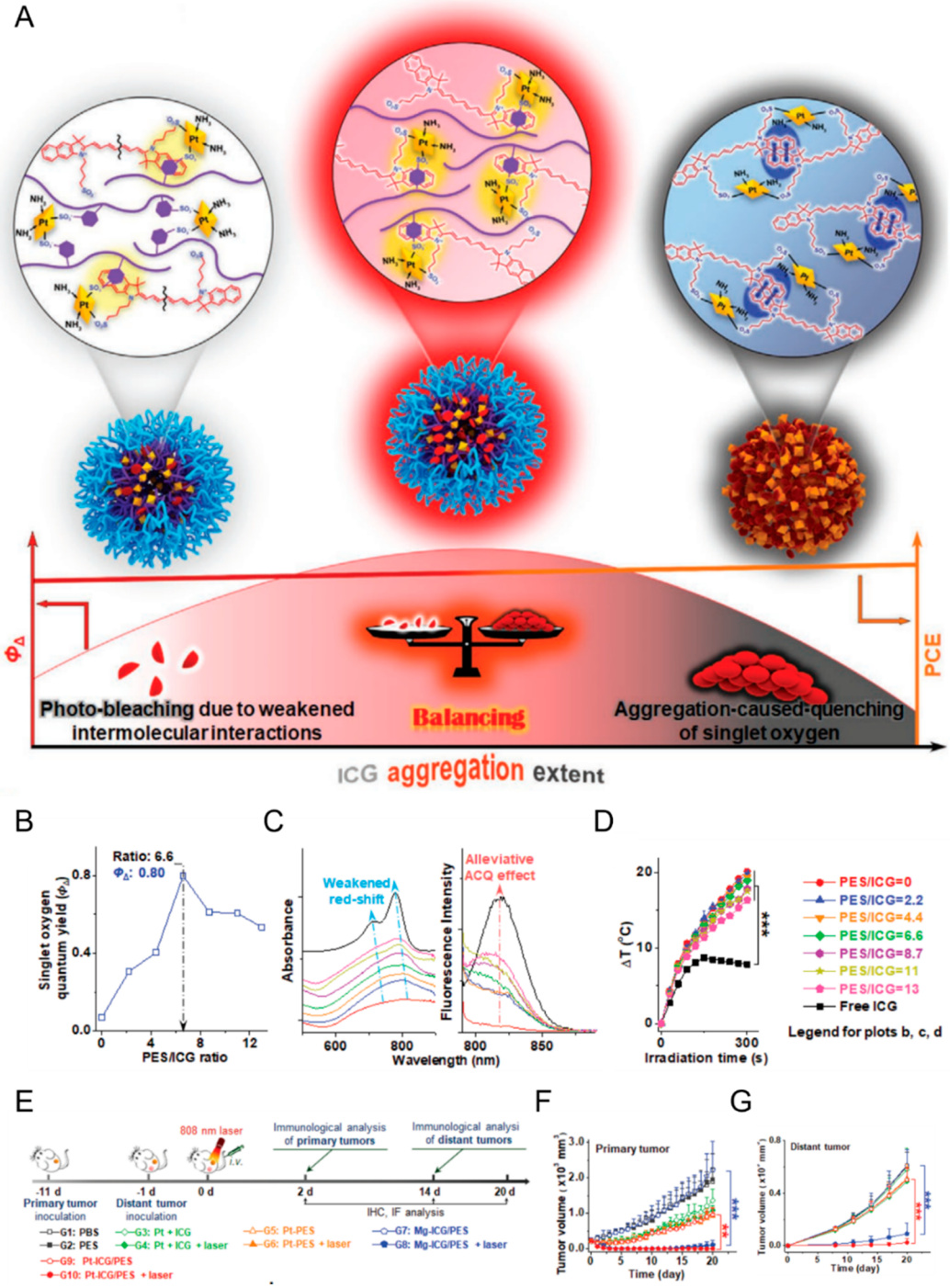

Figure 5. Schematic representation of discretely integrated nanoconstructs for PDT, PTT and cisplatin (Pt) chemotherapy. A. Discretely integrated nanoconstructs (DIN) containing ICG, cisplatin and polymeric spacer (PES) balance the desired photophysical properties, including singlet oxygen quantum yield (Φ_Δ) and aggregation-induced quenching. B. Singlet oxygen quantum yield of Pt-ICG/PES (ICG concentration 5.0 μg/mL) under 808 nm laser irradiation (1 W/cm^2, 5 min). The PES/ICG molar ratio was tuned by changing the feeding ratio of sulfonates in p(MEO2MA-co-OEGMA)-b-pSS (PES) and ICG. C. Absorption and emission spectra (λ_{ex}: 780 nm) of Pt-ICG/PES. D. Heat generation by Pt-ICG/PES (5 μg/mL of ICG) under 808 nm laser irradiation at 1 W/cm^2 for 5 min. E. Experimental design and timeline of Pt-ICG/PES-enabled PDT/PTT/chemotherapy treatment. Tumor growth curves of primary F. and distant G. 4T1 tumors in the immunocompetent BALB/c mice treated with systemically administered Pt + ICG, Pt-PES, Mg-ICG/PES and Pt-ICG/PES, with or without 808 nm laser treatment (1 W/cm^2, 10 min), mean ± SEM, n = 6. Adapted with permission from ref 184. Copyright 2022 Wiley-VCH GmbH.

fine-tuned through synthetic strategies. For example, a recent study by Wen et al. described polypyrrole - tellurophene nanoparticle synthesis by controlled oxidative copolymerization with $FeCl_3$.[200] Interestingly, the nanoparticle photothermal conversion efficiency directly correlated to the pyrrole content, while ROS generation was proportional to tellurophene content. The nanoparticles were simultaneously PDT- and PTT-active under a single 808 nm laser irradiation, as demonstrated by

https://doi.org/10.1021/acsnano.3c00891
ACS Nano 2023, 17, 7979−8003

successful treatment of 4T1 tumors *in vivo*. This and similar approaches can be used to design customizable formulations with the desired PDT and PTT properties.

Another interesting example of utilizing separate PDT and PTT components within a single nanoparticle is upconversion nanoparticle (UCNP)-based antigen-capturing nanoplatforms (Figure 6A).[201] UCNPs were utilized as a carrier, ICG as a light absorber for PTT, rose bengal as a photosensitizer and DSPE-PEG-maleimide as an antigen-capturing agent. Dual PDT/PTT treatment effectively decreased cell viability *in vitro* (Figure 6B)

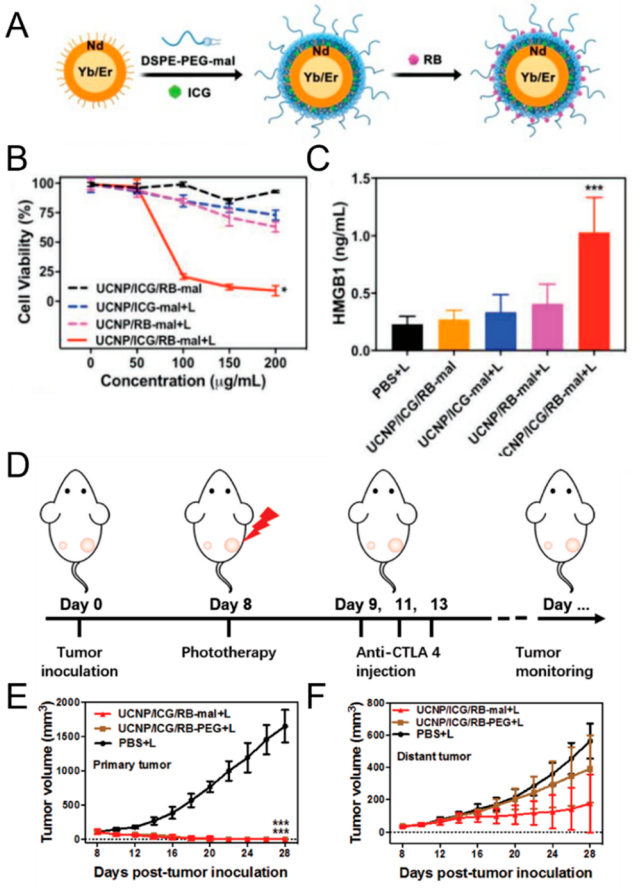

Figure 6. Schematic representation of an upconversion nanoparticle (UCNP)-based antigen-capturing nanoplatform (UCNP/ICG/RB-mal) for PDT/PTT treatment of metastatic breast cancer. A. UCNP/ICG/RB-mal synthesis. B. *In vitro* viability of 4T1 tumor cells incubated with different nanoparticles, followed by irradiation with an 805 nm laser (5 min, 0.75 W/cm^2). Nanoparticles integrating both photothermal (UCNP/ICG) and photodynamic (RB) components produced the greatest decrease in cell viability (*p < 0.05 vs UCNP/ICG/RB-mal group). C. Extracellular release of HMGB1 after different treatments (*p < 0.001 vs PBS + laser group). Data are expressed as means ± SD (n = 4). D. Experimental workflow investigating the abscopal effects UCNP/ICG/RB-mal based phototherapy combined with CTLA-4 immune checkpoint blockade. E. Growth curves of primary tumors of mice after various treatments demonstrate superior tumor growth control upon treatment with UCNP/ICG/RB-mal and light (***p < 0.001 vs PBS + laser group.) F. Growth curves of distant nodules in mice that received different treatments (mean ± SD, n = 5). Adapted with permission under a Creative Commons Attribution 4.0 International (CC BY 4.0) License from ref 201. Copyright 2019 Meng Wang et al., published by WILEY-VCH Verlag GmbH& Co. KGaA, Weinheim.**

and induced ICD, as demonstrated by the release of highly immunogenic HMGB1 (Figure 6C). DSPE-PEG-maleimide captured the released antigens *in situ*, facilitating activation of the local antigen-presenting cells, which led to robust antitumor immunity. Indeed, the combination of the dual PDT/PTT phototherapy with anti-CTLA 4 immunotherapy led to a delay in both primary and distant tumor growth in an orthotopic 4T1 BALB/c breast cancer model (Figure 6D−F).

Mesoporous silica nanoparticles offer wide-ranging possibilities for incorporating a variety of therapeutic agents due to their biocompatibility and large surface area. In a recent study, Goel et al. utilized mesoporous silica nanoshells to encapsulate CuS (as a PTT agent) and a *meso*-tetrakis(4-carboxyphenyl)porphyrin photosensitizer for PDT, yielding ^{89}Zr-labeled core−satellite nanohybrids (Figure 7A−C).[202] This design enabled synergistic PDT/PTT, wherein a single treatment completely eliminated tumors within 1 d (Figure 7D). Notably, the dual treatment was significantly superior to PDT (660 nm laser, no heat) or PTT (980 nm laser, T_{max} > 50 °C) alone, suggesting a synergistic rather than additive interaction.

Another approach involves combining photocatalytic titanium dioxide (TiO_2) or zinc oxide (ZnO) with plasmonic gold nanoparticles for light-induced ROS generation and localized heating.[203,204] A recent study leveraged site-specific placement of ICG at the ends of gold nanorods by growing porous TiO_2 caps to enhance singlet oxygen generation.[205] The surface plasmon resonance of gold nanoparticles was adjusted to overlap with the exciton absorption of ICG and DNA strands loaded with doxorubicin were attached to the gold nanorods sidewalls for simultaneous chemotherapy delivery. The synergistic effect of increased singlet oxygen and photothermal-induced drug delivery led to significant improvements in tumor cell killing, demonstrating the potential of this approach for hybrid PDT/PTT nanoparticle design.

Overall, there are several ways in which multifunctional phototheranostic agents will streamline the joint application of PDT and PTT (Table 3). In principle, it is possible to use two different agents to deliver simultaneous PDT and PTT. However, this is challenging in terms of achieving optimal relative tumor uptake, given the likely differences in pharmacokinetics and tumor localization. It is also complex from a regulatory perspective. Hence, it would be preferable to use a single agent that can serve as both a high light absorber for efficient PTT and have good singlet oxygen quantum yield for PDT. While, for example, ICG meets the former criterion, it has low singlet oxygen quantum yield and so is a poor PDT agent. Porphyrins show the converse, namely potential high singlet oxygen generation but relatively low efficiency for PTT. Nanoparticle formulations enable both properties to be achieved at the same time. At the cellular level, co-delivering a PS and a photothermal agent within a single nanoparticle has the potential to improve the interaction between the two modalities, resulting in multiple nonoverlapping cell death pathways. This can be further enhanced by loading a PDT/PTT-active nanoparticle with drugs, nucleic acids and immune-stimulating agents. Additionally, most nanoformulations offer a variety of multimodal imaging opportunities through the intrinsic properties of its components, such as fluorescence, CT contrast, magnetic properties, or through labeling with radioactive isotopes for positron emission tomography (PET) or (single-photon emission computed tomography (SPECT). Despite the variety of multifunctional agents found in the literature, only a handful demonstrate adequate pharmacokinetic and biodis-

https://doi.org/10.1021/acsnano.3c00891
ACS Nano 2023, 17, 7979−8003

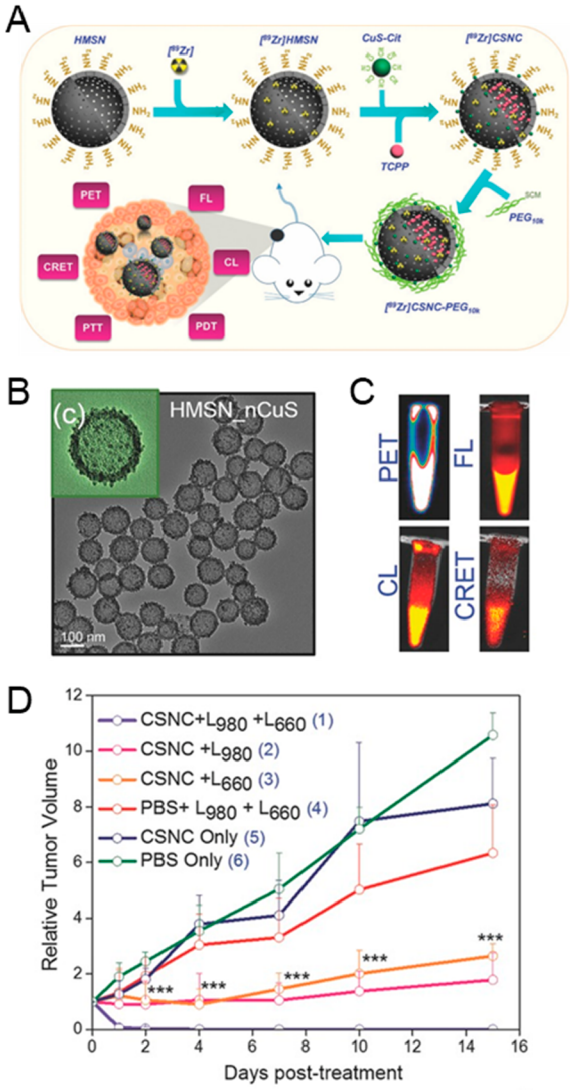

Figure 7. A. Schematic representation of a multifunctional core−satellite nanoconstructs (CSNCs) formulated by assembling CuS nanoparticles on the surface of [^{89}Zr]-labeled hollow mesoporous silica nanoshells containing porphyrin molecules and its use for multimodal cancer imaging and phototherapy. B. Transmission electron microscopy images of CSNCs at different magnifications. C. Representative positron emission tomography (PET), fluorescence (FL), Cerenkov luminescence (CL) and Cerenkov radiation energy transfer (CRET) images of radiolabeled CSNCs. D. Time-dependent tumor growth curves after various treatments (CSNC - core−satellite nanoconstruct, L980−980 nm laser irradiation for PTT, L630−630 nm laser for PDT, n = 5. Adapted with permission from ref 202. Copyright 2017 WILEY-VCH Verlag GmbH& Co. KGaA, Weinheim.

tribution properties *in vivo* for potential clinical translation. Agents that have a simple composition, robust synthesis and scale-up procedures and are PDT/PTT-active under a single wavelength are the most likely to reach clinical trials and facilitate clinical translation of PDT−PTT combination therapy.[202]

PRACTICAL AND TRANSLATIONAL ASPECTS OF PDT AND PTT COMBINATIONS

Both PDT and PTT require close coordination of several principal components, including possible exogenous photoabsorber administration, light source placement and light delivery parameters (fluence rate, fluence), as well as treatment response monitoring. This inherent complexity of multimodal treatments complicates their preclinical assessment and clinical implementation. The complexity increases when combining PDT and PTT, making it even more challenging to design preclinical studies and manage treatment logistics. Nevertheless, we believe that combining the robust PTT tissue coagulation with PDT tissue-sparing and immune-stimulating properties has significant clinical potential. In this, the use of dual-modality PDT/PTT-active nanoparticles simplifies treatment logistics and streamlines treatment planning. In this section we will discuss challenges in the context of PDT/PTT preclinical evaluation and outline our considerations regarding its clinical translation.

The choice of an external photoabsorber (or lack thereof) is a critical step in the treatment protocol design. In the simplest scenario, a single photoabsorber is used for both PDT and PTT, which are then conducted using the same light source and delivery system. This scenario allows PDT and PTT treatments to be performed simultaneously. However, sequential treatments may hold additional benefits, especially if one of the modalities is delivered at a low dose and is used to "prime" tumor for the subsequent treatment. For example, pretreating the tumor with subcoagulative PTT before PDT could stimulate reoxygenation and promote vascular leakiness, improving photosensitizer extravasation and hence the PDT efficacy. Likewise, subtherapeutic PDT treatment could improve tumor photoabsorber accumulation and increase tumor susceptibility to PTT. Alternatively, if the chosen photoabsorber acts as a PTT agent while intact and as a photosensitizer when disrupted, the treatment should be conducted sequentially during the experimentally established time points.[169] Many PDT/PTT active agents require two separate wavelengths for each modality. In this case, treatment is undertaken sequentially and the optimal choice of treatment order should be determined experimentally. For example, Kim et al. found that conducting PDT (655 nm) after PTT (808 nm) with gold nanorod-chlorin e6 nanogels did not bring any additional benefit compared to PTT only.[209] However, conducting PTT after PDT led to markedly improved tumor growth control. These results were likely due to PTT-induced vascular shutdown, which compromised tumor perfusion and negated the effects of the subsequent PDT. PTT, on the other hand, could be successfully conducted after PDT, since its cytotoxicity is largely oxygen-independent. In addition to selecting a suitable photoabsorber and establishing the order of treatments, the interval between treatments is extremely important. Finally, if PDT and PTT require different light sources, optimal fiber placement and light dosimetry need to be considered.

Another combination treatment that should be considered in addition to PDT/PTT is PDT combined with mild hyperthermia (Hx).[84,87,91,112] Clinically, Hx is used in conjunction with other treatment modalities, including chemotherapy and radiation. For example, hyperthermic intraperitoneal chemotherapy (HIPEC), during which a prewarmed chemotherapy solution is administered during surgery, is commonly applied to treat gastric and ovarian carcinomatosis as a means of enhancing chemotherapy efficacy.[219] Other methods of delivering hyperthermia locally include electromagnetic energy-induced heating, high-intensity focused ultrasound (HIFU) or magnetic hyperthermia.[220,221] There is a plethora of preclinical evidence in favor of PDT/Hx combination and, given the availability of clinical

https://doi.org/10.1021/acsnano.3c00891
ACS Nano 2023, 17, 7979−8003

Table 3. Summary of Recently Published PDT/PTT Nanoparticles Using Separate PDT and PTT Agents

PTT Agent	PDT Agent	Description	Tumor Model	Treatment Parameters	Ref
Gold NP	Chlorin e6	Chlorin e6-loaded plasmonic vesicular assemblies of gold nanoparticles	MDA-MB-435 SQ tumors, IT injection	PDT + PTT: 671 nm, 2 W/cm^2, 6 min (>42 °C)	206
		Chlorin e6-functionalized gold nanostars	MDAMB-435 SQ tumors, IT injection	PDT + PTT: 671 nm at 1.0 W/cm^2, 6 min (51.2 ± 1.4 °C)	207
		Polydopamine-coated gold nanoflowers conjugated with chlorin e6, η = 23.6%	SQ HeLa tumors, IT injection	PDT: 660 nm 100 mW/cm^2 10 min	208
				PTT: 808 nm, 2 W/cm^2, 10 min (55.1 °C)	
		Pluronic-based nanogel containing gold nanorods and chlorin e6	SCC7 SQ tumors; IV injection	PDT: 655 nm, 167 mW/cm^2, 20 J/cm^2	209
				PTT: 808 nm, 4 W/cm^2, 480 J/cm^2	
	ICG	Thermoresponsive mesoporous silica-coated gold nanorods incorporating ICG	A549 SQ tumors, IV injection	PDT + PTT: 808 nm laser at 0.8 W/cm^2, 3 min (41.2 °C)	210
		Gold NP and nanorods + ICG	*In vitro* only (A549 cells)	PDT + PTT: 808 nm laser, 20 W/cm^2, 2 min	211
		Au/MoS2-ICG Nanoplatform, η = 68.8%	HeLa SQ tumors, IT injection	PDT + PTT at 808 nm, 0.2 W/cm^2, 5 min	212
		ER-targeting ICG-conjugated hollow gold nanospheres + Hb-containing liposomes	CT-26 and B16 SQ tumor models	PDT + PTT at 808 nm laser, 1 W/cm^2, 2 min	213
	$AlPcS_4$	Gold nanorod- $AlPcS_4$ complex	SCC7 SQ tumors, IV injection	PDT: at 670 nm 331 mW/cm^2, 60 J/cm^2	196
				PTT: 810 nm laser, 3.82 W/cm^2, 229 J/cm^2 (65 °C)	
	MesoTetra (N -methyl-4-pyridyl) porphine tetrachloride	Collagen-based gold NP- $AlPcS_4$ hydrogel	MCF-7 SQ tumors, IT injection	PDT + PTT: 635 nm, 169.85 mW/cm^2, 10 min	214
Carbon NP	Chlorin e6	PEGylated graphene oxide loaded with chlorin e6	*In vitro* only (KB cells)	PDT: 660 nm laser, 50 mW/cm^2, 5 min, 15 J/cm^2	215
				PTT: 808 nm laser; 0.3 W/cm^2, 20 min, 360 J/cm^2	
	Methylene blue	Graphene oxide nanosheets functionalized with Pluronic block copolymer and complexed with methylene blue	HeLa SQ mouse model, IV injection	PDT: 650 nm, 150 mW/cm^2, 10 min	216
				PTT: 808 nm, 2 W/cm^2, 3 min	
MoS_2 nanosheets	Chlorin e6	Chlorin e6 surface-absorbed onto PEGylated MoS_2	4T1 SQ breast cancer model, IV injection	PDT: 660 nm laser, 5 mW cm^2, 20 min	217
				PTT: 808 nm laser, 0.45 W cm^2, 20 min	
Copper sulfide	Tetrakis (4-carboxyphenyl) porphyrin	CuS nanoparticles assembled on the surface of [^{89}Zr]-labeled hollow mesoporous silica nanoshells filled with porphyrin molecules	4T1 SQ breast cancer model, IV injection	PTT: 980 nm laser, 4 W/cm^2, 10 minPDT: 660 nm laser, 50 mW cm/cm^2, 20 min	202
Black phospohrus	Chlorin e6	Chlorin e6 (Ce6)-decorated BP nanosheets (NSs), η = 43.6%	HeLa SQ mouse model, IV injection	PDT + PTT: 660 nm, 0.65 W/cm^2, 10 min (46.8 °C)	218
Upconversion NP + ICG	Rose Bengal (RB)	ICG-coated upconversion nanoparticles loaded with RB	Orthotopic 4T1 tumors IT injection	PDT + PTT: 805 nm laser, 0.75 W/cm^2, 10 min (~60 °C)	201
Pyrrole	Tellurophene	Copolymer polypyrrole- tellurophene NPs, η = 31.3%−43.6%	4T1 SQ tumors, IV injection	PDP + PTT: with 808 nm laser, 1.5 W/cm^2, 10 min (49 °C)	200

https://doi.org/10.1021/acsnano.3c00891
ACS Nano 2023, 17, 7979−8003

protocols and devices to administer hyperthermia, this combination has a lower barrier to translation compared to combined PDT/PTT treatment at this time.

Finally, it is important to touch upon the importance of pursuing nanomaterials with established synthesis and scale-up approaches. Overall, nanoparticle manufacturing is achieved through "top-down", "bottom-up" processes, or their combinations.[222,223] Organic nanomaterials like liposomes, lipid or polymeric nanoparticles are typically formulated through "bottom-up" self-assembly, emulsification or precipitation. To achieve precise control over the size and morphology of a nanoparticle, these basic processes have been augmented by physical extrusion or rapid mixing, during which an ethanol phase (lipid components) and an aqueous phase (water-soluble components) are mixed under a certain pH and flow rate.[224−226] These methods have been perfected through decades of research culminating in the safe manufacturing of millions of lipid nanoparticle-based vaccines against severe acute respiratory syndrome coronavirus 2 (SARS-CoV-2).[224] The "top-down" approaches are becoming increasingly popular for the manufacturing of inorganic and biodegradable polymer nanoparticles with precisely controlled size distributions.[222] Photolithography is a widely used method of micropatterning in the semiconductor industry, during which a photosensitive film is illuminated with UV light applied through a photomask to introduce a micropattern to the desired surface. This method can be used to produce a variety of organic and inorganic materials, including hydrogels[227] and ferromagnetic particles.[228] Other "top-down" methods include nanoimprint lithography, microfluidics-based oil-in-water emulsion method and continuous flow lithography.[222] Adopting these methods is likely to improve experimental reproducibility and decrease batch-to-batch variability in nanoparticle morphology. For a more comprehensive description of "top-down" approaches, readers should refer to the recent review articles on the topic.[222,229]

PRECLINICAL CHALLENGES OF EVALUATING PDT AND PTT COMBINATIONS

The rapid development of nanotechnology has led to explosive growth in publications featuring multimodal nanomaterials. The growing interest in phototherapies has resulted in thousands of preclinical formulations that combine PDT and PTT properties. However, only a handful of phototherapeutic nanoparticles have reached clinical trials, including gold nanoshells[49] for PTT and liposomal benzoporphyrin derivative (Visudyne)[230,231] for PDT. Several trends in the literature may help explain such low translational success. First, most publications focus on characterizing the nanoparticle properties in solution and/or *in vitro*, with only a fraction evaluating the performance *in vivo*. Within those studies that do include *in vivo* experiments, only a few have evaluated the nanoparticle pharmacokinetics, biodistribution and therapeutic performance using intravenous injection. Most formulations, especially upconversion and carbon-based nanoparticles, can only produce meaningful therapeutic results using intratumoral injection, which is of limited clinical utility, and their long-term tissue retention and toxicity also remain of concern.[232,233] The focus on conceptual novelty and lack of attention to formulation optimization and thorough characterization prevent these preclinical advances from bridging the translational gap. Other common shortcomings in nanoparticle design are the complexity of formulation and the use of a large number of nanoparticle components. Formulation complexity complicates characterization and scale-up, often leading to irreproducible results.[234] One way of overcoming this is by following a "one-for-all" paradigm,[235] wherein a single nanoparticle building block possesses multiple intrinsic functionalities. Furthermore, there is an increased interest in all-organic formulations that can serve as both PDT and PTT agent simultaneously under a single wavelength irradiation. This relieves the toxicity concerns associated with the use of inorganic nanoparticles, simplifies treatment logistics as treatment can be conduced using a single light source/delivery system and facilitates clinical translation. Successful preclinical examples of this approach include porphysomes,[167] nanodots[186] and several peptide- and polymer-based formulations.[154]

Another challenge in PDT/PTT preclinical studies is quantifying the interaction between the two modalities and ensuring the appropriate selection of controls. While most preclinical studies discussed in this review abide formally by the rule of including separate PDT, PTT, PDT + PTT and control arms, several caveats often remain overlooked. The experiment must account for the effects of each therapy alone to distinguish additive from synergistic interactions. However, distinguishing the effects of PDT from PTT is not trivial, especially if treatment is conducted using a dual-modality photoabsorber and a single activation wavelength. Several common approaches include using equivalent doses of monomeric photosensitizer/PTT agent, designing control formulations with PDT-only or PTT-only properties, or using external factors that negate either PDT or PTT effects. Surrogate approaches can also be used to separately mimic the effects of PDT and PTT. For example, high-intensity focused ultrasound or water bath heating may be used to produce heat in a controlled manner in the absence of exogenous photoabsorbers. While these methods may not fully recapitulate the PTT effects, they can provide a useful reference. Similarly, PDT-induced ROS effects may, to a certain extent, be mimicked by radiation therapy, a complication being that other forms of the radiation-induced damage need to be considered.

Using monomers or individual nanoparticle components as controls seldom allows for a proper assessment of the effects of each modality in isolation. For example, using a monomer photosensitizer in a PDT-only control arm would negate any quenching present within hybrid PDT/PTT nanoparticles. Furthermore, monomers typically have different biodistribution and pharmacokinetics compared to nanoparticles, so that its intratumoral concentration may not be representative of that in the PDT/PTT nanoparticle arm. Designing separate PDT-only and PTT-only nanoparticle controls can be adequate if certain conditions are fulfilled. First, control formulations must have the same absorption coefficients as the original PDT/PTT nanoparticle at their corresponding PDT and PTT wavelengths. Excluding a photosensitizer from a nanoparticle formulation may decrease its absorbance, resulting in less potent heating than in the PDT/PTT arm. Second, control nanoparticles must exhibit comparable pharmacokinetics and biodistribution as the original formulation. Lastly, control formulations should have equivalent photothermal conversion efficiency or ROS quenching to the dual PDT/PTT agent.

In some cases, designing adequate control formulations is impossible. However, several additional tools are available that allow separating PDT effects from PTT effects. These cannot fully replace traditional controls but may provide valuable mechanistic insights. One way of mimicking PDT conditions is by conducting PTT treatment in multiple short interrupted cycles that prevent tissue from heating.[175] This strategy, while it

https://doi.org/10.1021/acsnano.3c00891
ACS Nano 2023, 17, 7979−8003

has drawbacks, can be helpful to get an idea of how strong the PDT effects are when conducted simultaneously with PTT using the same wavelength and laser power. Another common strategy that can minimize PDT effects during combined treatment is by adding a ROS scavenger, such as NaN_3[207] or vitamin C.[187,194] This can provide valuable insights into the mechanisms of action, provided that PTT + scavenger controls are also included. Various degrees of ROS generation have been demonstrated during PTT, so that including an inhibitor may not only negate the PDT effect but also artifactually decrease the PTT cytotoxicity. Alternatively, PDT effects may be minimized by conducting the treatment in a hypoxic environment.[173] Finally, some studies use active cooling to minimize PTT effects during PDT.[187]

TRANSLATIONAL CONSIDERATIONS

Dual PDT/PTT treatment involves the use of drug-device combinations, which are relatively more complex compared to mono treatments. Availability and cost of light sources, laser fibers, endoscopic equipment, as well as the need for imaging guidance, temperature monitoring and online dosimetry should all be considered during PDT/PTT treatment planning. In cases when either PDT or PTT is expected to produce an acceptable response, dual PDT/PTT treatment may not be justifiable. For example, if an adequate treatment dose can be delivered throughout an entire tumor volume with either PDT or PTT (>55 °C) alone, their immediate treatment outcomes are often comparable and the use of the combination treatment may not be necessary.[1] Well-vascularized superficial tumors that are highly responsive to PDT, such as skin, esophagus and bladder lesions, are unlikely to benefit from introducing PTT treatment. Moreover, PDT and/or PTT may already be combined with other clinical modalities, such as chemotherapy, surgery or radiation, which creates additional translational considerations. However, it is worthwhile exploring PDT/PTT combinations in tumors that cannot be treated safely or effectively with either modality alone. Within this framework, we consider several scenarios in which the joint application of PDT and PTT may be beneficial.

The two main safety concerns in PDT and PTT are systemic photosensitivity and the lack of heat confinement, respectively. There are several ways in which combination treatments could lessen these safety concerns. First, simultaneous PTT−PDT application may decrease the PTT target volume and laser power required to achieve tumor regression. In this case, PDT can be used to selectively target the tumor periphery and infiltrative tumor components, while sparing the surrounding tissues. Sequential treatment may be used to reduce the PTT target volume, for example, by using PTT to photocoagulate the (hypoxic) tumor core and PDT to target the infiltrative tumor regions.

In many cases, PTT cannot be used due to concerns about thermal damage to the surrounding anatomical structures, including blood vessels, ECM scaffolds and nerves. In this scenario, combining with PDT would allow the target coagulation volume and the required laser power to be reduced. Within this framework, we will highlight two cancer types in which we believe the combination of PDT and PTT may be beneficial − pancreatic and colorectal cancers.

Pancreatic cancer is one of the few cancer types that has not seen a significant improvement in the 5-year survival rates for decades, currently ∼9%.[236] The only curative option is surgery followed by adjuvant chemotherapy; however, only 30% of patients have resectable tumors. Surgical resection of pancreatic cancer is complicated by its anatomical location, typically the head of the pancreas that is in close proximity to the duodenum, portal vein and aorta. Hence, minimally invasive and tissue-sparing options are urgently needed. Several phase I and I/II clinical trials have demonstrated the technical feasibility of PDT in inoperable pancreatic cancer.[230,237,238] In this approach, several optical fibers were percutaneously placed under CT, ultrasound or endoscopic ultrasound guidance. While these trials demonstrated acceptable safety profile and dose-dependent tumor necrosis, the treatment responses were highly variable, which could be explained, at least in part, by hypoxia, a known hallmark of pancreatic cancer. Thus, supplementing PDT with oxygen-independent PTT could decrease the rates of local recurrence without compromising safety. Various modes of thermal ablation have also been explored in pancreatic cancer, including laser, radiofrequency, microwave and high-intensity ultrasound ablation.[239] However, the safe ablation volume is limited by the surrounding sensitive structures. Using subablative PTT (<55 °C) in conjunction with PDT could enhance the efficacy, while also leveraging the tissue-sparing and ECM-preserving capabilities of PDT.

Colorectal cancer is in the top three leading causes of cancer-associated deaths and the incidence is on the rise worldwide.[240] Depending on the anatomical location, preventing colon perforation and preserving the anal sphincter to avoid a permanent colostomy are high priorities. Several clinical studies have evaluated the feasibility of PDT for colorectal cancer detection and treatment. For example, Sun et al. investigated Photofrin PDT in 23 patients with advanced colorectal cancer,[241] with treatment conducted in 2 fractions, each of ∼12 min irradiation at 200 J/cm^2 (630 nm). Necrotic tissue was removed endoscopically between treatments. The response rate in the PDT group was 69.57% compared to 40% in patients who received standard-of-care radiation and chemotherapy only. Furthermore, the rate of adverse effects, including changes in bowel behavior, hematochezia intestinal stimulation and incomplete intestinal obstruction, were significantly less frequent after PDT. This study, however, was performed in advanced cases with metastatic spread, which likely contributed to the modest increase in overall survival benefit of PDT (6.23 ± 1.65 months *versus* 3.01 ± 1.12 months). We hypothesize that PDT or PDT/PTT combination treatment could produce better results in patients with localized disease while maintaining minimal scaring and with minimal adverse effects, thereby significantly improving quality of life. Photothermal ablation also has been investigated in patients with pulmonary[242] and liver[243] metastases of colorectal cancer but was never performed in primary colorectal tumors due to safety concerns. Combining PDT with PTT- or Hx-range heating regimens could increase the PDT treatment efficacy and overcome hypoxia.

Another way of considering PDT/PTT combinations comes from analyzing the more established area of hyperthermia-radiation treatments. Both PDT and radiation therapy rely on oxygen-dependent ROS production and so face common treatment challenges. Cases of successful combination of hyperthermia and radiation can then help define the clinical scenarios in which PDT/PTT combinations could be helpful. For example, the successes in treating locally advanced colorectal and cervical cancers using hyperthermia and radiation provide an additional indication that this type of cancer would be responsive to PDT/PTT.[244]

https://doi.org/10.1021/acsnano.3c00891
ACS Nano 2023, 17, 7979−8003

SUMMARY

This review article is intended to provide a broad overview of various ways in which PDT/PTT interactions can occur and how nanotechnology presents opportunities for combining these approaches. A detailed understanding of the cellular, tumor microenvironmental and pharmacokinetic factors is necessary for the design of clinically translatable agents that could leverage the synergy between PDT and PTT. Here, we have highlighted several promising developments in the design of dual PDT- and PTT-active nanomaterials and considered how external photoabsorbers may influence treatment planning. It is hoped that this will stimulate discussion of the preclinical challenges in evaluating the interaction between PDT and PTT as well as opportunities and challenges in translating this combination into clinical practice.

AUTHOR INFORMATION

Corresponding Author

Gang Zheng − *Princess Margaret Cancer Centre, University Health Network, Toronto, Ontario M5G 1L7, Canada; Department of Medical Biophysics and Institute of Biomaterials and Biomedical Engineering, University of Toronto, Toronto, Ontario M5G 1L7, Canada;* orcid.org/0000-0002-0705-7398; Email: gang.zheng@uhnres.utoronto.ca

Authors

Marta Overchuk − *Princess Margaret Cancer Centre, University Health Network, Toronto, Ontario M5G 1L7, Canada; Joint Department of Biomedical Engineering, University of North Carolina at Chapel Hill and North Carolina State University, Chapel Hill, North Carolina 27599, United States*

Robert A. Weersink − *Princess Margaret Cancer Centre, University Health Network, Toronto, Ontario M5G 1L7, Canada; Department of Medical Biophysics, Institute of Biomaterials and Biomedical Engineering, and Department of Radiation Oncology, University of Toronto, Toronto, Ontario M5G 1L7, Canada*

Brian C. Wilson − *Princess Margaret Cancer Centre, University Health Network, Toronto, Ontario M5G 1L7, Canada; Department of Medical Biophysics, University of Toronto, Toronto, Ontario M5G 1L7, Canada*

Complete contact information is available at: https://pubs.acs.org/10.1021/acsnano.3c00891

Notes

The authors declare no competing financial interest.

ACKNOWLEDGMENTS

The authors thank Dr. Adam Koebel for designing and preparing Figures [1], [2] and the graphical abstract. The authors also acknowledge funding support from the Terry Fox Research Institute (PPG #1075), the Canadian Institute for Health Research (FDN154326), the Canada Research Chairs Program (950-232468) and the Princess Margaret Cancer Foundation.

VOCABULARY

Photodynamic therapy uses visible to near-infrared light (<200 mW) and photosensitizers to generate reactive oxygen species at the site of irradiation. The biological effects of photodynamic therapy include reactive oxygen species-mediated cell death, vascular damage and inflammation and are strictly nonthermal. Photodynamic therapy has been explored in the clinic for a variety of cancers and premalignant conditions, including skin, esophageal, bladder, lung, brain and prostate.

Photothermal therapy exploits relatively high-power lasers (up to 10 W) to induce localized tumor heating. It can be divided into subcoagulative PTT (43−55 °C), and coagulative PTT (55−60 °C), which leads to irreversible changes through rapid tissue photocoagulation. Photothermal therapy can rely on the endogenous tissue light absorption or make use of external photoabsorbers to enhance localized heating.

Photothermal ablation uses high-energy lasers to remove tissue from the surface as an alternative to surgical resection. It has been explored for resection of liver, bladder and colorectal cancers, among others.

Photosensitizers are natural or synthetic molecules that absorb light of a suitable wavelength and transfer photon energy to other molecules via photodynamic reaction. This typically results in the generation of cytotoxic singlet oxygen or free radicals. Examples of clinically approved photosensitizer include porfimer sodium (Photofrin), aminolevulinic acid and benzoporphyrin derivative (Visudyne).

Photoabsorber is defined as an agent with a high light-to-heat conversion efficiency that is used to enhance the local light-based heating of target tissues.

Synergy is the type of interaction between two treatments that produces a combined effect greater than the sum of their separate effects.

REFERENCES

(1) Wilson, B. C.; Weersink, R. A. The Yin and Yang of PDT and PTT. *Photochem. Photobiol.* **2020**, *96* (2), 219−231.

(2) Li, X.; Lovell, J. F.; Yoon, J.; Chen, X. Clinical development and potential of photothermal and photodynamic therapies for cancer. *Nat. Rev. Clin Oncol* **2020**, *17* (11), 657−674.

(3) Nunes, T.; Hamdan, D.; Leboeuf, C.; El Bouchtaoui, M.; Gapihan, G.; Nguyen, T. T.; Meles, S.; Angeli, E.; Ratajczak, P.; Lu, H.; Di Benedetto, M.; Bousquet, G.; Janin, A. Targeting Cancer Stem Cells to Overcome Chemoresistance. *Int. J. Mol. Sci.* **2018**, *19* (12), 4036.

(4) Spring, B. Q.; Rizvi, I.; Xu, N.; Hasan, T. The role of photodynamic therapy in overcoming cancer drug resistance. *Photochem. Photobiol. Sci.* **2015**, *14* (8), 1476−91.

(5) Huang, H. C.; Rizvi, I.; Liu, J.; Anbil, S.; Kalra, A.; Lee, H.; Baglo, Y.; Paz, N.; Hayden, D.; Pereira, S.; Pogue, B. W.; Fitzgerald, J.; Hasan, T. Photodynamic Priming Mitigates Chemotherapeutic Selection Pressures and Improves Drug Delivery. *Cancer Res.* **2018**, *78* (2), 558−571.

(6) Hauck, T. S.; Jennings, T. L.; Yatsenko, T.; Kumaradas, J. C.; Chan, W. C. W. Enhancing the Toxicity of Cancer Chemotherapeutics with Gold Nanorod Hyperthermia. *Adv. Mater.* **2008**, *20* (20), 3832−3838.

(7) Fay, B. L.; Melamed, J. R.; Day, E. S. Nanoshell-mediated photothermal therapy can enhance chemotherapy in inflammatory breast cancer cells. *Int. J. Nanomedicine* **2015**, *10*, 6931−41.

(8) Rizvi, I.; Celli, J. P.; Evans, C. L.; Abu-Yousif, A. O.; Muzikansky, A.; Pogue, B. W.; Finkelstein, D.; Hasan, T. Synergistic enhancement of carboplatin efficacy with photodynamic therapy in a three-dimensional model for micrometastatic ovarian cancer. *Cancer Res.* **2010**, *70* (22), 9319−28.

(9) Snyder, J. W.; Greco, W. R.; Bellnier, D. A.; Vaughan, L.; Henderson, B. W. Photodynamic therapy: a means to enhanced drug delivery to tumors. *Cancer Res.* **2003**, *63* (23), 8126−31.

(10) Gao, W.; Wang, Z.; Lv, L.; Yin, D.; Chen, D.; Han, Z.; Ma, Y.; Zhang, M.; Yang, M.; Gu, Y. Photodynamic Therapy Induced Enhancement of Tumor Vasculature Permeability Using an Upcon-

version Nanoconstruct for Improved Intratumoral Nanoparticle Delivery in Deep Tissues. *Theranostics* **2016**, *6* (8), 1131−44.
(11) Overchuk, M.; Harmatys, K. M.; Sindhwani, S.; Rajora, M. A.; Koebel, A.; Charron, D. M.; Syed, A. M.; Chen, J.; Pomper, M. G.; Wilson, B. C.; Chan, W. C. W.; Zheng, G. Subtherapeutic Photodynamic Treatment Facilitates Tumor Nanomedicine Delivery and Overcomes Desmoplasia. *Nano Lett.* **2021**, *21* (1), 344−352.
(12) Raeesi, V.; Chan, W. C. Improving nanoparticle diffusion through tumor collagen matrix by photo-thermal gold nanorods. *Nanoscale* **2016**, *8* (25), 12524−30.
(13) Chen, B.; Pogue, B. W.; Luna, J. M.; Hardman, R. L.; Hoopes, P. J.; Hasan, T. Tumor vascular permeabilization by vascular-targeting photosensitization: effects, mechanism, and therapeutic implications. *Clin. Cancer Res.* **2006**, *12* (3), 917−923.
(14) Kim, M. M.; Darafsheh, A. Light Sources and Dosimetry Techniques for Photodynamic Therapy. *Photochem. Photobiol.* **2020**, *96* (2), 280−294.
(15) Shafirstein, G.; Bellnier, D.; Oakley, E.; Hamilton, S.; Potasek, M.; Beeson, K.; Parilov, E. Interstitial Photodynamic Therapy-A Focused Review. *Cancers (Basel)* **2017**, *9* (2), 12.
(16) Pogue, B. W.; Elliott, J. T.; Kanick, S. C.; Davis, S. C.; Samkoe, K. S.; Maytin, E. V.; Pereira, S. P.; Hasan, T. Revisiting photodynamic therapy dosimetry: reductionist & surrogate approaches to facilitate clinical success. *Phys. Med. Biol.* **2016**, *61* (7), R57−89.
(17) Agostinis, P.; Berg, K.; Cengel, K. A.; Foster, T. H.; Girotti, A. W.; Gollnick, S. O.; Hahn, S. M.; Hamblin, M. R.; Juzeniene, A.; Kessel, D.; Korbelik, M.; Moan, J.; Mroz, P.; Nowis, D.; Piette, J.; Wilson, B. C.; Golab, J. Photodynamic therapy of cancer: an update. *CA Cancer J. Clin* **2011**, *61* (4), 250−81.
(18) Juarranz, A.; Jaen, P.; Sanz-Rodriguez, F.; Cuevas, J.; Gonzalez, S. Photodynamic therapy of cancer. Basic principles and applications. *Clin Transl Oncol* **2008**, *10* (3), 148−54.
(19) Wilson, B. C.; Patterson, M. S. The physics, biophysics and technology of photodynamic therapy. *Phys. Med. Biol.* **2008**, *53* (9), R61−109.
(20) Baptista, M. S.; Cadet, J.; Di Mascio, P.; Ghogare, A. A.; Greer, A.; Hamblin, M. R.; Lorente, C.; Nunez, S. C.; Ribeiro, M. S.; Thomas, A. H.; Vignoni, M.; Yoshimura, T. M. Type I and Type II Photosensitized Oxidation Reactions: Guidelines and Mechanistic Pathways. *Photochem. Photobiol.* **2017**, *93* (4), 912−919.
(21) Sharman, W. M.; Allen, C. M.; van Lier, J. E. Role of activated oxygen species in photodynamic therapy. *Methods Enzymol* **2000**, *319*, 376−400.
(22) Monro, S.; Colon, K. L.; Yin, H.; Roque, J., 3rd; Konda, P.; Gujar, S.; Thummel, R. P.; Lilge, L.; Cameron, C. G.; McFarland, S. A. Transition Metal Complexes and Photodynamic Therapy from a Tumor-Centered Approach: Challenges, Opportunities, and Highlights from the Development of TLD1433. *Chem. Rev.* **2019**, *119* (2), 797−828.
(23) Mo, J.; Mai Le, N. P.; Priefer, R. Evaluating the mechanisms of action and subcellular localization of ruthenium(II)-based photosensitizers. *Eur. J. Med. Chem.* **2021**, *225*, 113770.
(24) Chitgupi, U.; Qin, Y.; Lovell, J. F. Targeted Nanomaterials for Phototherapy. *Nanotheranostics* **2017**, *1* (1), 38−58.
(25) Betz, C. S.; Jager, H. R.; Brookes, J. A.; Richards, R.; Leunig, A.; Hopper, C. Interstitial photodynamic therapy for a symptom-targeted treatment of complex vascular malformations in the head and neck region. *Lasers Surg Med.* **2007**, *39* (7), 571−82.
(26) de Visscher, S. A.; Melchers, L. J.; Dijkstra, P. U.; Karakullukcu, B.; Tan, I. B.; Hopper, C.; Roodenburg, J. L.; Witjes, M. J. mTHPC-mediated photodynamic therapy of early stage oral squamous cell carcinoma: a comparison to surgical treatment. *Ann. Surg Oncol* **2013**, *20* (9), 3076−82.
(27) Dole, K. C.; Chen, Q.; Hetzel, F. W.; Whalen, L. R.; Blanc, D.; Huang, Z. Effects of photodynamic therapy on peripheral nerve: in situ compound-action potentials study in a canine model. *Photomed Laser Surg* **2005**, *23* (2), 172−6.
(28) Kubler, A. C.; Stenzel, W.; Ruhling, M.; Meul, B.; Fischer, J. H. Experimental evaluation of possible side effects of intra-operative photodynamic therapy on rabbit blood vessels and nerves. *Lasers Surg Med.* **2003**, *33* (4), 247−55.
(29) Barr, H.; Tralau, C. J.; Boulos, P. B.; MacRobert, A. J.; Tilly, R.; Bown, S. G. The contrasting mechanisms of colonic collagen damage between photodynamic therapy and thermal injury. *Photochem. Photobiol.* **1987**, *46* (5), 795−800.
(30) Civantos, F. J.; Karakullukcu, B.; Biel, M.; Silver, C. E.; Rinaldo, A.; Saba, N. F.; Takes, R. P.; Vander Poorten, V.; Ferlito, A. A Review of Photodynamic Therapy for Neoplasms of the Head and Neck. *Adv. Ther* **2018**, *35* (3), 324−340.
(31) Filonenko, E. V.; Kaprin, A. D.; Alekseev, B. Y.; Apolikhin, O. I.; Slovokhodov, E. K.; Ivanova-Radkevich, V. I.; Urlova, A. N. 5-Aminolevulinic acid in intraoperative photodynamic therapy of bladder cancer (results of multicenter trial). *Photodiagnosis Photodyn Ther* **2016**, *16*, 106−109.
(32) Yano, T.; Hatogai, K.; Morimoto, H.; Yoda, Y.; Kaneko, K. Photodynamic therapy for esophageal cancer. *Ann. Transl Med.* **2014**, *2* (3), 29.
(33) Overholt, B. F.; Wang, K. K.; Burdick, J. S.; Lightdale, C. J.; Kimmey, M.; Nava, H. R.; Sivak, M. V., Jr.; Nishioka, N.; Barr, H.; Marcon, N.; Pedrosa, M.; Bronner, M. P.; Grace, M.; Depot, M. Five-year efficacy and safety of photodynamic therapy with Photofrin in Barrett's high-grade dysplasia. *Gastrointest Endosc* **2007**, *66* (3), 460−8.
(34) Simone, C. B., 2nd; Cengel, K. A. Photodynamic therapy for lung cancer and malignant pleural mesothelioma. *Semin Oncol* **2014**, *41* (6), 820−30.
(35) Kato, H.; Harada, M.; Ichinose, S.; Usuda, J.; Tsuchida, T.; Okunaka, T. Photodynamic therapy (PDT) of lung cancer: experience of the Tokyo Medical University. *Photodiagnosis Photodyn Ther* **2004**, *1* (1), 49−55.
(36) Azzouzi, A. R.; Emberton, M. Padeliporfin vascular-targeted photodynamic therapy versus active surveillance in men with low-risk prostate cancer - Authors' reply. *Lancet Oncol.* **2017**, *18* (4), No. e188.
(37) Fan, B. G.; Andren-Sandberg, A. Photodynamic therapy for pancreatic cancer. *Pancreas* **2007**, *34* (4), 385−9.
(38) Pattani, V. P.; Shah, J.; Atalis, A.; Sharma, A.; Tunnell, J. W. Role of apoptosis and necrosis in cell death induced by nanoparticle-mediated photothermal therapy. *J. Nanopart. Res.* **2015**, *17* (1), 1−11.
(39) Tong, L.; Zhao, Y.; Huff, T. B.; Hansen, M. N.; Wei, A.; Cheng, J. X. Gold Nanorods Mediate Tumor Cell Death by Compromising Membrane Integrity. *Adv. Mater.* **2007**, *19*, 3136−3141.
(40) Dickson, J. A.; Calderwood, S. K. Temperature range and selective sensitivity of tumors to hyperthermia: a critical review. *Ann. N.Y. Acad. Sci.* **1980**, *335*, 180−205.
(41) Stapleton, S.; Dunne, M.; Milosevic, M.; Tran, C. W.; Gold, M. J.; Vedadi, A.; McKee, T. D.; Ohashi, P. S.; Allen, C.; Jaffray, D. A. Radiation and Heat Improve the Delivery and Efficacy of Nanotherapeutics by Modulating Intratumoral Fluid Dynamics. *ACS Nano* **2018**, *12* (8), 7583−7600.
(42) Richter, K.; Haslbeck, M.; Buchner, J. The heat shock response: life on the verge of death. *Mol. Cell* **2010**, *40* (2), 253−66.
(43) Bown, S. G. Endoscopic laser therapy for oesophageal cancer. *Endoscopy* **1986**, *18* (Suppl 3), 26−31.
(44) Urschel, J. D.; Cockburn, J. S.; Foote, A. V. Palliation of oesophageal cancer–endoscopic intubation and laser therapy. *Postgrad Med. J.* **1991**, *67* (787), 414−6.
(45) Wenger, H.; Yousuf, A.; Oto, A.; Eggener, S. Laser ablation as focal therapy for prostate cancer. *Curr. Opin Urol* **2014**, *24* (3), 236−40.
(46) Gough-Palmer, A. L.; Gedroyc, W. M. Laser ablation of hepatocellular carcinoma–a review. *World J. Gastroenterol* **2008**, *14* (47), 7170−4.
(47) Bozinov, O.; Yang, Y.; Oertel, M. F.; Neidert, M. C.; Nakaji, P. Laser interstitial thermal therapy in gliomas. *Cancer Lett.* **2020**, *474*, 151−157.
(48) Patel, P.; Patel, N. V.; Danish, S. F. Intracranial MR-guided laser-induced thermal therapy: single-center experience with the Visualase thermal therapy system. *J. Neurosurg* **2016**, *125* (4), 853−860.
(49) Rastinehad, A. R.; Anastos, H.; Wajswol, E.; Winoker, J. S.; Sfakianos, J. P.; Doppalapudi, S. K.; Carrick, M. R.; Knauer, C. J.;

https://doi.org/10.1021/acsnano.3c00891
ACS Nano 2023, 17, 7979−8003

Taouli, B.; Lewis, S. C.; Tewari, A. K.; Schwartz, J. A.; Canfield, S. E.; George, A. K.; West, J. L.; Halas, N. J. Gold nanoshell-localized photothermal ablation of prostate tumors in a clinical pilot device study. *Proc. Natl. Acad. Sci. U. S. A.* **2019**, *116* (37), 18590−18596.
(50) Schwartzberg, B.; Lewin, J.; Abdelatif, O.; Bernard, J.; Bu-Ali, H.; Cawthorn, S.; Chen-Seetoo, M.; Feldman, S.; Govindarajulu, S.; Jones, L.; Juette, A.; Kavia, S.; Maganini, R.; Pain, S.; Shere, M.; Shriver, C.; Smith, S.; Valencia, A.; Whitacre, E.; Whitney, R. Phase 2 Open-Label Trial Investigating Percutaneous Laser Ablation for Treatment of Early-Stage Breast Cancer: MRI, Pathology, and Outcome Correlations. *Ann. Surg Oncol* **2018**, *25* (10), 2958−2964.
(51) Li, X.; Ferrel, G. L.; Guerra, M. C.; Hode, T.; Lunn, J. A.; Adalsteinsson, O.; Nordquist, R. E.; Liu, H.; Chen, W. R. Preliminary safety and efficacy results of laser immunotherapy for the treatment of metastatic breast cancer patients. *Photochem. Photobiol. Sci.* **2011**, *10* (5), 817−21.
(52) Ivan, K.; Robert, W.; Brian, W. Photoacoustic methods for direct monitoring of nanoparticle enhanced photothermal ablation in biological tissues: visualizing scattering, absorption, and thermal effects. *Proc. SPIE* **2022**, *12216*, No. 122160E.
(53) Li, C. L.; Fisher, C. J.; Wilson, B. C.; Weersink, R. A., Preclinical evaluation of a clinical prototype transrectal diffuse optical tomography system for monitoring photothermal therapy of focal prostate cancer. *J. Biomed. Opt.* **2022**, *27* (2). DOI: 10.1117/1.JBO.27.2.026001.
(54) Kolesnikov, I. E.; Kurochkin, M. A.; Meshkov, I. N.; Akasov, R. A.; Kalinichev, A. A.; Kolesnikov, E. Y.; Gorbunova, Y. G.; Lähderanta, E. Water-soluble multimode fluorescent thermometers based on porphyrins photosensitizers. *Materials & Design* **2021**, *203*, 109613.
(55) Qiao, J.; Li, X.; Qi, L. Fluorescent polymer-modified gold nanobipyramids for temperature sensing during photothermal therapy in living cells. *Chin. Chem. Lett.* **2022**, *33* (6), 3193−3196.
(56) Espinosa, A.; Castro, G. R.; Reguera, J.; Castellano, C.; Castillo, J.; Camarero, J.; Wilhelm, C.; García, M. A.; Muñoz-Noval, Á. Photoactivated Nanoscale Temperature Gradient Detection Using X-ray Absorption Spectroscopy as a Direct Nanothermometry Method. *Nano Lett.* **2021**, *21* (1), 769−777.
(57) Kessel, D.; Oleinick, N. L. Cell Death Pathways Associated with Photodynamic Therapy: An Update. *Photochem. Photobiol.* **2018**, *94* (2), 213−218.
(58) Kessel, D. Critical PDT Theory III: Events at the Molecular and Cellular Level. *Int. J. Mol. Sci.* **2022**, *23* (11), 6195.
(59) Kessel, D.; Luo, Y.; Deng, Y.; Chang, C. K. The role of subcellular localization in initiation of apoptosis by photodynamic therapy. *Photochem. Photobiol.* **1997**, *65* (3), 422−6.
(60) Liu, X.; Kim, C. N.; Yang, J.; Jemmerson, R.; Wang, X. Induction of apoptotic program in cell-free extracts: requirement for dATP and cytochrome c. *Cell* **1996**, *86* (1), 147−57.
(61) Rickard, B. P.; Overchuk, M.; Obaid, G.; Ruhi, M. K.; Demirci, U.; Fenton, S. E.; Santos, J. H.; Kessel, D.; Rizvi, I. Photochemical Targeting of Mitochondria to Overcome Chemoresistance in Ovarian Cancer(dagger). *Photochem. Photobiol.* **2023**, *99*, 448.
(62) Kessel, D.; Reiners, J. J., Jr Enhanced efficacy of photodynamic therapy via a sequential targeting protocol. *Photochem. Photobiol.* **2014**, *90* (4), 889−895.
(63) Rizvi, I.; Obaid, G.; Bano, S.; Hasan, T.; Kessel, D. Photodynamic therapy: Promoting in vitro efficacy of photodynamic therapy by liposomal formulations of a photosensitizing agent. *Lasers Surg Med.* **2018**, *50* (5), 499−505.
(64) Kim, H. R.; Luo, Y.; Li, G.; Kessel, D. Enhanced apoptotic response to photodynamic therapy after bcl-2 transfection. *Cancer Res.* **1999**, *59* (14), 3429−3432.
(65) Kessel, D. Photodynamic therapy: apoptosis, paraptosis and beyond. *Apoptosis* **2020**, *25* (9−10), 611−615.
(66) Garg, A. D.; Krysko, D. V.; Vandenabeele, P.; Agostinis, P. DAMPs and PDT-mediated photo-oxidative stress: exploring the unknown. *Photochem. Photobiol. Sci.* **2011**, *10* (5), 670−80.
(67) Nath, S.; Obaid, G.; Hasan, T. The Course of Immune Stimulation by Photodynamic Therapy: Bridging Fundamentals of Photochemically Induced Immunogenic Cell Death to the Enrichment of T-Cell Repertoire. *Photochem. Photobiol.* **2019**, *95* (6), 1288−1305.
(68) Garg, A. D.; Agostinis, P. ER stress, autophagy and immunogenic cell death in photodynamic therapy-induced anti-cancer immune responses. *Photochem. Photobiol. Sci.* **2014**, *13* (3), 474−87.
(69) Beltran Hernandez, I.; Angelier, M. L.; Del Buono D'Ondes, T.; Di Maggio, A.; Yu, Y.; Oliveira, S. The Potential of Nanobody-Targeted Photodynamic Therapy to Trigger Immune Responses. *Cancers (Basel)* **2020**, *12* (4), 978.
(70) Chen, B.; Xu, Y.; Agostinis, P.; De Witte, P. A. Synergistic effect of photodynamic therapy with hypericin in combination with hyperthermia on loss of clonogenicity of RIF-1 cells. *Int. J. Oncol.* **2001**, *18* (6), 1279−1285.
(71) Kinsey, J.; Cortese, D.; Neel, H. Thermal considerations in murine tumor killing using hematoporphyrin derivative phototherapy. *Cancer Res.* **1983**, *43* (4), 1562−1567.
(72) Svaasand, L. O.; Doiron, D. R.; Dougherty, T. J. Temperature rise during photoradiation therapy of malignant tumors. *Med. Phys.* **1983**, *10* (1), 10−7.
(73) Perez-Hernandez, M.; Del Pino, P.; Mitchell, S. G.; Moros, M.; Stepien, G.; Pelaz, B.; Parak, W. J.; Galvez, E. M.; Pardo, J.; de la Fuente, J. M. Dissecting the molecular mechanism of apoptosis during photothermal therapy using gold nanoprisms. *ACS Nano* **2015**, *9* (1), 52−61.
(74) Melamed, J. R.; Edelstein, R. S.; Day, E. S. Elucidating the fundamental mechanisms of cell death triggered by photothermal therapy. *ACS Nano* **2015**, *9* (1), 6−11.
(75) Zhang, Y.; Zhan, X.; Xiong, J.; Peng, S.; Huang, W.; Joshi, R.; Cai, Y.; Liu, Y.; Li, R.; Yuan, K.; Zhou, N.; Min, W. Temperature-dependent cell death patterns induced by functionalized gold nanoparticle photothermal therapy in melanoma cells. *Sci. Rep.* **2018**, *8* (1), 8720.
(76) Patel, N. V.; Frenchu, K.; Danish, S. F. Does the Thermal Damage Estimate Correlate With the Magnetic Resonance Imaging Predicted Ablation Size After Laser Interstitial Thermal Therapy? *Oper Neurosurg (Hagerstown)* **2018**, *15* (2), 179−183.
(77) Raz, O.; Haider, M. A.; Davidson, S. R.; Lindner, U.; Hlasny, E.; Weersink, R.; Gertner, M. R.; Kucharcyzk, W.; McCluskey, S. A.; Trachtenberg, J. Real-time magnetic resonance imaging-guided focal laser therapy in patients with low-risk prostate cancer. *Eur. Urol* **2010**, *58* (1), 173−7.
(78) Ashrafi, A. N.; Nassiri, N.; Gill, I. S.; Gulati, M.; Park, D.; de Castro Abreu, A. L. Contrast-Enhanced Transrectal Ultrasound in Focal Therapy for Prostate Cancer. *Curr. Urol. Rep.* **2018**, *19* (10), 87.
(79) Atri, M.; Gertner, M. R.; Haider, M. A.; Weersink, R. A.; Trachtenberg, J. Contrast-enhanced ultrasonography for real-time monitoring of interstitial laser thermal therapy in the focal treatment of prostate cancer. *Can. Urol. Assoc. J.* **2009**, *3* (2), 125−30.
(80) He, J.; Li, C. L.; Wilson, B. C.; Fisher, C. J.; Ghai, S.; Weersink, R. A. A Clinical Prototype Transrectal Diffuse Optical Tomography (TRDOT) System for In vivo Monitoring of Photothermal Therapy (PTT) of Focal Prostate Cancer. *IEEE Trans. Biomed. Eng.* **2020**, *67* (7), 2119−2129.
(81) Geoghegan, R.; Ter Haar, G.; Nightingale, K.; Marks, L.; Natarajan, S. Methods of monitoring thermal ablation of soft tissue tumors - A comprehensive review. *Med. Phys.* **2022**, *49* (2), 769−791.
(82) Chin, L. C.; Whelan, W. M.; Vitkin, I. A. Models and measurements of light intensity changes during laser interstitial thermal therapy: implications for optical monitoring of the coagulation boundary location. *Phys. Med. Biol.* **2003**, *48* (4), 543−59.
(83) Christensen, T.; Wahl, A.; Smedshammer, L. Effects of haematoporphyrin derivative and light in combination with hyperthermia on cells in culture. *Br. J. Cancer* **1984**, *50* (1), 85−9.
(84) Hirschberg, H.; Sun, C. H.; Tromberg, B. J.; Yeh, A. T.; Madsen, S. J. Enhanced cytotoxic effects of 5-aminolevulinic acid-mediated photodynamic therapy by concurrent hyperthermia in glioma spheroids. *J. Neurooncol* **2004**, *70* (3), 289−99.
(85) Bienia, A.; Wiechec-Cudak, O.; Murzyn, A. A.; Krzykawska-Serda, M. Photodynamic Therapy and Hyperthermia in Combination

Treatment-Neglected Forces in the Fight against Cancer. *Pharmaceutics* **2021**, *13* (8), 1147.
(86) Orenstein, A.; Kostenich, G.; Kopolovic, Y.; Babushkina, T.; Malik, Z. Enhancement of ALA-PDT Damage by IR-lnduced Hyperthermia on a Colon Carcinoma Model. *Photochem. Photobiol.* **1999**, *69* (6), 703−707.
(87) Kelleher, D.; Bastian, J.; Thews, O.; Vaupel, P. Enhanced effects of aminolaevulinic acid-based photodynamic therapy through local hyperthermia in rat tumours. *British journal of cancer* **2003**, *89* (2), 405−411.
(88) Chen, B.; Roskams, T.; de Witte, P. A. Enhancing the antitumoral effect of hypericin-mediated photodynamic therapy by hyperthermia. *Lasers in surgery and medicine* **2002**, *31* (3), 158−163.
(89) Rasch, M. H.; Tijssen, K.; VanSteveninck, J.; Dubbelman, T. M. Synergistic interaction of photodynamic treatment with the sensitizer aluminum phthalocyanine and hyperthermia on loss of clonogenicity of CHO cells. *Photochem. Photobiol.* **1996**, *64* (3), 586−93.
(90) Mang, T. S. Combination studies of hyperthermia induced by the neodymium: yttrium-aluminum-garnet (Nd:YAG) laser as an adjuvant to photodynamic therapy. *Lasers Surg Med.* **1990**, *10* (2), 173−8.
(91) Henderson, B. W.; Waldow, S. M.; Potter, W. R.; Dougherty, T. J. Interaction of photodynamic therapy and hyperthermia: tumor response and cell survival studies after treatment of mice in vivo. *Cancer Res.* **1985**, *45* (12), 6071−6077.
(92) Hiraoka, M.; Hahn, G. M. Comparison between tumor pH and cell sensitivity to heat in RIF-1 tumors. *Cancer Res.* **1989**, *49* (14), 3734−3736.
(93) Prinsze, C.; Penning, L. C.; Dubbelman, T. M.; VanSteveninck, J. Interaction of photodynamic treatment and either hyperthermia or ionizing radiation and of ionizing radiation and hyperthermia with respect to cell killing of L929 fibroblasts, Chinese hamster ovary cells, and T24 human bladder carcinoma cells. *Cancer Res.* **1992**, *52* (1), 117−120.
(94) Abrahamse, H.; Hamblin, M. R. New photosensitizers for photodynamic therapy. *Biochem. J.* **2016**, *473* (4), 347−64.
(95) van der Heijden, A. G.; Dewhirst, M. W. Effects of hyperthermia in neutralising mechanisms of drug resistance in non-muscle-invasive bladder cancer. *Int. J. Hyperthermia* **2016**, *32* (4), 434−45.
(96) Borys, N.; Dewhirst, M. W. Drug development of lyso-thermosensitive liposomal doxorubicin: Combining hyperthermia and thermosensitive drug delivery. *Adv. Drug Deliv Rev.* **2021**, *178*, 113985.
(97) Kurokawa, H.; Ito, H.; Terasaki, M.; Matsui, H. Hyperthermia enhances photodynamic therapy by regulation of HCP1 and ABCG2 expressions via high level ROS generation. *Sci. Rep.* **2019**, *9* (1), 1638.
(98) Lee, W. H.; Lee, J. M.; Lim, C.; Kim, S.; Kim, S. G. Structural requirements within protoporphyrin IX in the inhibition of heat shock protein 90. *Chem. Biol. Interact* **2013**, *204* (1), 49−57.
(99) Arba, M.; Ruslin, R.; Kartasasmita, R. E.; Surantaatmadja, S. I.; Tjahjono, D. H. Insight into the Interaction of Cationic Porphyrin-Anthraquinone Hybrids with Hsp90: In Silico Analysis. *J. MATH. FUNDAMENTAL SCI.* **2018**, *50* (3), 303−314.
(100) Tang, Z.; Zhao, P.; Ni, D.; Liu, Y.; Zhang, M.; Wang, H.; Zhang, H.; Gao, H.; Yao, Z.; Bu, W. Pyroelectric nanoplatform for NIR-II-triggered photothermal therapy with simultaneous pyroelectric dynamic therapy. *Materials Horizons* **2018**, *5* (5), 946−952.
(101) Horsman, M. R. Tissue physiology and the response to heat. *Int. J. Hyperthermia* **2006**, *22* (3), 197−203.
(102) Iwata, K.; Shakil, A.; Hur, W. J.; Makepeace, C. M.; Griffin, R. J.; Song, C. W. Tumour pO2 can be increased markedly by mild hyperthermia. *Br. J. Cancer Suppl.* **1996**, *27*, S217−S221.
(103) Gu, Y.; Chen, W. R.; Xia, M.; Jeong, S. W.; Liu, H. Effect of photothermal therapy on breast tumor vascular contents: noninvasive monitoring by near-infrared spectroscopy. *Photochem. Photobiol.* **2005**, *81* (4), 1002−1009.
(104) Kong, G.; Braun, R. D.; Dewhirst, M. W. Hyperthermia enables tumor-specific nanoparticle delivery: effect of particle size. *Cancer Res.* **2000**, *60* (16), 4440−4445.
(105) Melancon, M. P.; Elliott, A. M.; Shetty, A.; Huang, Q.; Stafford, R. J.; Li, C. Near-infrared light modulated photothermal effect increases vascular perfusion and enhances polymeric drug delivery. *J. Controlled Release* **2011**, *156* (2), 265−72.
(106) van Leeuwen-van Zaane, F.; de Bruijn, H. S.; van der Ploeg-van den Heuvel, A.; Sterenborg, H. J.; Robinson, D. J. The effect of fluence rate on the acute response of vessel diameter and red blood cell velocity during topical 5-aminolevulinic acid photodynamic therapy. *Photodiagnosis Photodyn Ther* **2014**, *11* (2), 71−81.
(107) Becker, T. L.; Paquette, A. D.; Keymel, K. R.; Henderson, B. W.; Sunar, U. Monitoring blood flow responses during topical ALA-PDT. *Biomed Opt Express* **2011**, *2* (1), 123−30.
(108) Fingar, V. H.; Kik, P. K.; Haydon, P. S.; Cerrito, P. B.; Tseng, M.; Abang, E.; Wieman, T. J. Analysis of acute vascular damage after photodynamic therapy using benzoporphyrin derivative (BPD). *Br. J. Cancer* **1999**, *79* (11−12), 1702−8.
(109) Krammer, B. Vascular effects of photodynamic therapy. *Anticancer Res.* **2001**, *21* (6B), 4271−4277.
(110) He, C.; Agharkar, P.; Chen, B. Intravital microscopic analysis of vascular perfusion and macromolecule extravasation after photodynamic vascular targeting therapy. *Pharm. Res.* **2008**, *25* (8), 1873−80.
(111) Kimel, S.; Svaasand, L.; Hammer-Wilson, M.; Gottfried, V.; Cheng, S.; Svaasand, E.; Berns, M. Demonstration of synergistic effects of hyperthermia and photodynamic therapy using the chick chorioallantoic membrane model. *Lasers in surgery and medicine* **1992**, *12* (4), 432−440.
(112) Kelleher, D. K.; Thews, O.; Scherz, A.; Salomon, Y.; Vaupel, P. Combined hyperthermia and chlorophyll-based photodynamic therapy: tumour growth and metabolic microenvironment. *Br. J. Cancer* **2003**, *89* (12), 2333−9.
(113) Hu, Q.; Huang, Z.; Duan, Y.; Fu, Z.; Bin, L. Reprogramming Tumor Microenvironment with Photothermal Therapy. *Bioconjug Chem.* **2020**, *31* (5), 1268−1278.
(114) Theocharis, A. D.; Skandalis, S. S.; Gialeli, C.; Karamanos, N. K. Extracellular matrix structure. *Adv. Drug Deliv Rev.* **2016**, *97*, 4−27.
(115) Schaefer, L.; Schaefer, R. M. Proteoglycans: from structural compounds to signaling molecules. *Cell Tissue Res.* **2010**, *339* (1), 237−46.
(116) Provenzano, P. P.; Hingorani, S. R. Hyaluronan, fluid pressure, and stromal resistance in pancreas cancer. *Br. J. Cancer* **2013**, *108* (1), 1−8.
(117) Abyaneh, H. S.; Regenold, M.; McKee, T. D.; Allen, C.; Gauthier, M. A. Towards extracellular matrix normalization for improved treatment of solid tumors. *Theranostics* **2020**, *10* (4), 1960−1980.
(118) Chauhan, V. P.; Boucher, Y.; Ferrone, C. R.; Roberge, S.; Martin, J. D.; Stylianopoulos, T.; Bardeesy, N.; DePinho, R. A.; Padera, T. P.; Munn, L. L.; Jain, R. K. Compression of pancreatic tumor blood vessels by hyaluronan is caused by solid stress and not interstitial fluid pressure. *Cancer Cell* **2014**, *26* (1), 14−5.
(119) Yokoi, K.; Kojic, M.; Milosevic, M.; Tanei, T.; Ferrari, M.; Ziemys, A. Capillary-wall collagen as a biophysical marker of nanotherapeutic permeability into the tumor microenvironment. *Cancer Res.* **2014**, *74* (16), 4239−46.
(120) Barr, H.; Tralau, C. J.; MacRobert, A. J.; Krasner, N.; Boulos, P. B.; Clark, C. G.; Bown, S. G. Photodynamic therapy in the normal rat colon with phthalocyanine sensitisation. *Br. J. Cancer* **1987**, *56* (2), 111−8.
(121) Kolosnjaj-Tabi, J.; Marangon, I.; Nicolas-Boluda, A.; Silva, A. K. A.; Gazeau, F. Nanoparticle-based hyperthermia, a local treatment modulating the tumor extracellular matrix. *Pharmacol. Res.* **2017**, *126*, 123−137.
(122) Marangon, I.; Silva, A. A.; Guilbert, T.; Kolosnjaj-Tabi, J.; Marchiol, C.; Natkhunarajah, S.; Chamming's, F.; Menard-Moyon, C.; Bianco, A.; Gennisson, J. L.; Renault, G.; Gazeau, F. Tumor Stiffening, a Key Determinant of Tumor Progression, is Reversed by Nanomaterial-Induced Photothermal Therapy. *Theranostics* **2017**, *7* (2), 329−343.
(123) Barr, H.; MacRobert, A. J.; Tralau, C. J.; Boulos, P. B.; Bown, S. G. The significance of the nature of the photosensitizer for photodynamic therapy: quantitative and biological studies in the colon. *Br. J. Cancer* **1990**, *62* (5), 730−5.

https://doi.org/10.1021/acsnano.3c00891
ACS Nano 2023, 17, 7979−8003

(124) Queiros, C.; Garrido, P. M.; Maia Silva, J.; Filipe, P. Photodynamic therapy in dermatology: Beyond current indications. *Dermatol. Ther.* **2020**, *33* (6), e13997.
(125) Nelson, J. S.; Liaw, L. H.; Orenstein, A.; Roberts, W. G.; Berns, M. W. Mechanism of tumor destruction following photodynamic therapy with hematoporphyrin derivative, chlorin, and phthalocyanine. *J. Natl. Cancer Inst* **1988**, *80* (20), 1599−605.
(126) Obaid, G.; Bano, S.; Mallidi, S.; Broekgaarden, M.; Kuriakose, J.; Silber, Z.; Bulin, A. L.; Wang, Y.; Mai, Z.; Jin, W.; Simeone, D.; Hasan, T. Impacting Pancreatic Cancer Therapy in Heterotypic in Vitro Organoids and in Vivo Tumors with Specificity-Tuned, NIR-Activable Photoimmunonanoconjugates: Towards Conquering Desmoplasia? *Nano Lett.* **2019**, *19* (11), 7573−7587.
(127) Saad, M. A.; Zhung, W.; Stanley, M. E.; Formica, S.; Grimaldo-Garcia, S.; Obaid, G.; Hasan, T. Photoimmunotherapy Retains Its Anti-Tumor Efficacy with Increasing Stromal Content in Heterotypic Pancreatic Cancer Spheroids. *Mol. Pharmaceutics* **2022**, *19* (7), 2549−2563.
(128) Obaid, G.; Bano, S.; Thomsen, H.; Callaghan, S.; Shah, N.; Swain, J. W. R.; Jin, W.; Ding, X.; Cameron, C. G.; McFarland, S. A.; Wu, J.; Vangel, M.; Stoilova-McPhie, S.; Zhao, J.; Mino-Kenudson, M.; Lin, C.; Hasan, T. Remediating Desmoplasia with EGFR-Targeted Photoactivable Multi-Inhibitor Liposomes Doubles Overall Survival in Pancreatic Cancer. *Adv. Sci. (Weinh)* **2022**, *9* (24), e2104594.
(129) Kobayashi, H.; Furusawa, A.; Rosenberg, A.; Choyke, P. L. Near-infrared photoimmunotherapy of cancer: a new approach that kills cancer cells and enhances anti-cancer host immunity. *Int. Immunol.* **2021**, *33* (1), 7−15.
(130) Falk-Mahapatra, R.; Gollnick, S. O. Photodynamic Therapy and Immunity: An Update. *Photochem. Photobiol.* **2020**, *96* (3), 550−559.
(131) Anand, S.; Chan, T. A.; Hasan, T.; Maytin, E. V. Current Prospects for Treatment of Solid Tumors via Photodynamic, Photothermal, or Ionizing Radiation Therapies Combined with Immune Checkpoint Inhibition (A Review). *Pharmaceuticals (Basel)* **2021**, *14* (5), 447.
(132) Yan, G.; Shi, L.; Zhang, F.; Luo, M.; Zhang, G.; Liu, P.; Liu, K.; Chen, W. R.; Wang, X. Transcriptomic analysis of mechanism of melanoma cell death induced by photothermal therapy. *J. Biophotonics* **2021**, *14* (8), No. e202100034.
(133) Sweeney, E. E.; Cano-Mejia, J.; Fernandes, R. Photothermal Therapy Generates a Thermal Window of Immunogenic Cell Death in Neuroblastoma. *Small* **2018**, *14* (20), No. e1800678.
(134) Duan, X.; Chan, C.; Guo, N.; Han, W.; Weichselbaum, R. R.; Lin, W. Photodynamic Therapy Mediated by Nontoxic Core-Shell Nanoparticles Synergizes with Immune Checkpoint Blockade To Elicit Antitumor Immunity and Antimetastatic Effect on Breast Cancer. *J. Am. Chem. Soc.* **2016**, *138* (51), 16686−16695.
(135) Lou, J.; Aragaki, M.; Bernards, N.; Chee, T.; Gregor, A.; Hiraishi, Y.; Ishiwata, T.; Leung, C.; Ding, L.; Kitazawa, S.; Koga, T.; Sata, Y.; Ogawa, H.; Chen, J.; Kato, T.; Yasufuku, K.; Zheng, G. Repeated photodynamic therapy mediates the abscopal effect through multiple innate and adaptive immune responses with and without immune checkpoint therapy. *Biomaterials* **2023**, *292*, 121918.
(136) Lou, J.; Aragaki, M.; Bernards, N.; Kinoshita, T.; Mo, J.; Motooka, Y.; Ishiwata, T.; Gregor, A.; Chee, T.; Chen, Z.; Chen, J.; Kaga, K.; Wakasa, S.; Zheng, G.; Yasufuku, K. Repeated porphyrin lipoprotein-based photodynamic therapy controls distant disease in mouse mesothelioma via the abscopal effect. *Nanophotonics* **2021**, *10* (12), 3279−3294.
(137) Nagaya, T.; Friedman, J.; Maruoka, Y.; Ogata, F.; Okuyama, S.; Clavijo, P. E.; Choyke, P. L.; Allen, C.; Kobayashi, H. Host Immunity Following Near-Infrared Photoimmunotherapy Is Enhanced with PD-1 Checkpoint Blockade to Eradicate Established Antigenic Tumors. *Cancer Immunol Res.* **2019**, *7* (3), 401−413.
(138) Ghosh, S.; He, X.; Huang, W. C.; Lovell, J. F. Immune checkpoint blockade enhances chemophototherapy in a syngeneic pancreatic tumor model. *APL Bioeng* **2022**, *6* (3), No. 036105.
(139) Lou, J.; Zhang, L.; Zheng, G. Advancing Cancer Immunotherapies with Nanotechnology. *Advanced Therapeutics* **2019**, *2* (4), 1800128.
(140) Zhang, Z.; Sang, W.; Xie, L.; Li, W.; Li, B.; Li, J.; Tian, H.; Yuan, Z.; Zhao, Q.; Dai, Y. Polyphenol-Based Nanomedicine Evokes Immune Activation for Combination Cancer Treatment. *Angew. Chem., Int. Ed. Engl.* **2021**, *60* (4), 1967−1975.
(141) Xie, Z.; Peng, M.; Lu, R.; Meng, X.; Liang, W.; Li, Z.; Qiu, M.; Zhang, B.; Nie, G.; Xie, N.; Zhang, H.; Prasad, P. N. Black phosphorus-based photothermal therapy with aCD47-mediated immune checkpoint blockade for enhanced cancer immunotherapy. *Light Sci. Appl.* **2020**, *9*, 161.
(142) Li, J.; Xie, L.; Li, B.; Yin, C.; Wang, G.; Sang, W.; Li, W.; Tian, H.; Zhang, Z.; Zhang, X.; Fan, Q.; Dai, Y. Engineering a Hydrogen-Sulfide-Based Nanomodulator to Normalize Hyperactive Photothermal Immunogenicity for Combination Cancer Therapy. *Adv. Mater.* **2021**, *33* (22), No. e2008481.
(143) Adnan, A.; Munoz, N. M.; Prakash, P.; Habibollahi, P.; Cressman, E. N. K.; Sheth, R. A. Hyperthermia and Tumor Immunity. *Cancers (Basel)* **2021**, *13*, 11.
(144) Wan Mohd Zawawi, W. F. A.; Hibma, M. H.; Salim, M. I.; Jemon, K. Hyperthermia by near infrared radiation induced immune cells activation and infiltration in breast tumor. *Sci. Rep.* **2021**, *11* (1), 10278.
(145) Li, Z.; Deng, J.; Sun, J.; Ma, Y. Hyperthermia Targeting the Tumor Microenvironment Facilitates Immune Checkpoint Inhibitors. *Front Immunol* **2020**, *11*, 595207.
(146) Kadkhoda, J.; Tarighatnia, A.; Barar, J.; Aghanejad, A.; Davaran, S. Recent advances and trends in nanoparticles based photothermal and photodynamic therapy. *Photodiagnosis Photodyn Ther* **2022**, *37*, 102697.
(147) Matsumura, Y.; Maeda, H. A new concept for macromolecular therapeutics in cancer chemotherapy: mechanism of tumoritropic accumulation of proteins and the antitumor agent smancs. *Cancer Res.* **1986**, *46* (12), 6387−6392.
(148) Overchuk, M.; Zheng, G. Overcoming obstacles in the tumor microenvironment: Recent advancements in nanoparticle delivery for cancer theranostics. *Biomaterials* **2018**, *156*, 217−237.
(149) Xie, J.; Wang, Y.; Choi, W.; Jangili, P.; Ge, Y.; Xu, Y.; Kang, J.; Liu, L.; Zhang, B.; Xie, Z.; He, J.; Xie, N.; Nie, G.; Zhang, H.; Kim, J. S. Overcoming barriers in photodynamic therapy harnessing nano-formulation strategies. *Chem. Soc. Rev.* **2021**, *50* (16), 9152−9201.
(150) Ng, K. K.; Zheng, G. Molecular Interactions in Organic Nanoparticles for Phototheranostic Applications. *Chem. Rev.* **2015**, *115* (19), 11012−42.
(151) Rajora, M. A.; Lou, J. W. H.; Zheng, G. Advancing porphyrin's biomedical utility via supramolecular chemistry. *Chem. Soc. Rev.* **2017**, *46* (21), 6433−6469.
(152) Albanese, A.; Tang, P. S.; Chan, W. C. The effect of nanoparticle size, shape, and surface chemistry on biological systems. *Annu. Rev. Biomed Eng.* **2012**, *14*, 1−16.
(153) Kumari, S.; Sharma, N.; Sahi, S. V. Advances in Cancer Therapeutics: Conventional Thermal Therapy to Nanotechnology-Based Photothermal Therapy. *Pharmaceutics* **2021**, *13* (8), 1174.
(154) Zhao, L.; Liu, Y.; Chang, R.; Xing, R.; Yan, X. Supramolecular Photothermal Nanomaterials as an Emerging Paradigm toward Precision Cancer Therapy. *Adv. Funct. Mater.* **2019**, *29* (4), 1806877.
(155) Huang, X.; Jain, P. K.; El-Sayed, I. H.; El-Sayed, M. A. Plasmonic photothermal therapy (PPTT) using gold nanoparticles. *Lasers Med. Sci.* **2008**, *23* (3), 217−28.
(156) Luo, M.; Fan, T.; Zhou, Y.; Zhang, H.; Mei, L. 2D Black Phosphorus−Based Biomedical Applications. *Adv. Funct. Mater.* **2019**, *29* (13), 1808306.
(157) Dias, L. D.; Buzzá, H. H.; Stringasci, M. D.; Bagnato, V. S. Recent Advances in Combined Photothermal and Photodynamic Therapies against Cancer Using Carbon Nanomaterial Platforms for In Vivo Studies. *Photochem* **2021**, *1* (3), 434−447.
(158) Yin, F.; Hu, K.; Chen, S.; Wang, D.; Zhang, J.; Xie, M.; Yang, D.; Qiu, M.; Zhang, H.; Li, Z. G. Black phosphorus quantum dot based

https://doi.org/10.1021/acsnano.3c00891
ACS Nano 2023, 17, 7979−8003

novel siRNA delivery systems in human pluripotent teratoma PA-1 cells. *J. Mater. Chem. B* **2017**, *5* (27), 5433−5440.
(159) Tang, Z.; Kong, N.; Ouyang, J.; Feng, C.; Kim, N. Y.; Ji, X.; Wang, C.; Farokhzad, O. C.; Zhang, H.; Tao, W. Phosphorus Science-Oriented Design and Synthesis of Multifunctional Nanomaterials for Biomedical Applications. *Matter* **2020**, *2* (2), 297−322.
(160) Zhu, Y.; Xie, Z.; Li, J.; Liu, Y.; Li, C.; Liang, W.; Huang, W.; Kang, J.; Cheng, F.; Kang, L.; Al-Hartomy, O. A.; Al-Ghamdi, A.; Wageh, S.; Xu, J.; Li, D.; Zhang, H. From phosphorus to phosphorene: Applications in disease theranostics. *Coord. Chem. Rev.* **2021**, *446*, 214110.
(161) Wang, Y.; Qiu, M.; Won, M.; Jung, E.; Fan, T.; Xie, N.; Chi, S.-G.; Zhang, H.; Kim, J. S. Emerging 2D material-based nanocarrier for cancer therapy beyond graphene. *Coord. Chem. Rev.* **2019**, *400*, 213041.
(162) Kim, M.; Lee, J. H.; Nam, J. M. Plasmonic Photothermal Nanoparticles for Biomedical Applications. *Adv. Sci. (Weinh)* **2019**, *6* (17), 1900471.
(163) Zhou, J.; Rao, L.; Yu, G.; Cook, T. R.; Chen, X.; Huang, F. Supramolecular cancer nanotheranostics. *Chem. Soc. Rev.* **2021**, *50* (4), 2839−2891.
(164) Rajora, M. A.; Lou, J. W. H.; Zheng, G. Advancing porphyrin's biomedical utility via supramolecular chemistry. *Chem. Soc. Rev.* **2017**, *46* (21), 6433−6469.
(165) Huynh, E.; Zheng, G. Engineering multifunctional nanoparticles: all-in-one versus one-for-all. *Wiley Interdiscip Rev. Nanomed Nanobiotechnol* **2013**, *5* (3), 250−65.
(166) Zhao, M.; Zeng, Q.; Li, X.; Xing, D.; Zhang, T. Aza-BODIPY-based phototheranostic nanoagent for tissue oxygen auto-adaptive photodynamic/photothermal complementary therapy. *Nano Research* **2022**, *15* (1), 716−727.
(167) Lovell, J. F.; Jin, C. S.; Huynh, E.; Jin, H.; Kim, C.; Rubinstein, J. L.; Chan, W. C.; Cao, W.; Wang, L. V.; Zheng, G. Porphysome nanovesicles generated by porphyrin bilayers for use as multimodal biophotonic contrast agents. *Nat. Mater.* **2011**, *10* (4), 324−32.
(168) Jin, C. S.; Overchuk, M.; Cui, L.; Wilson, B. C.; Bristow, R. G.; Chen, J.; Zheng, G. Nanoparticle-Enabled Selective Destruction of Prostate Tumor Using MRI-Guided Focal Photothermal Therapy. *Prostate* **2016**, *76* (13), 1169−1181.
(169) Guidolin, K.; Ding, L.; Chen, J.; Wilson, B. C.; Zheng, G. Porphyrin-lipid nanovesicles (Porphysomes) are effective photosensitizers for photodynamic therapy. *Nanophotonics* **2021**, *10* (12), 3161−3168.
(170) Philp, L.; Chan, H.; Rouzbahman, M.; Overchuk, M.; Chen, J.; Zheng, G.; Bernardini, M. Q. Use of Porphysomes to detect primary tumour, lymph node metastases, intra-abdominal metastases and as a tool for image-guided lymphadenectomy: proof of concept in endometrial cancer. *Theranostics* **2019**, *9* (9), 2727−2738.
(171) Jin, C. S.; Wada, H.; Anayama, T.; McVeigh, P. Z.; Hu, H. P.; Hirohashi, K.; Nakajima, T.; Kato, T.; Keshavjee, S.; Hwang, D.; Wilson, B. C.; Zheng, G.; Yasufuku, K. An Integrated Nanotechnology-Enabled Transbronchial Image-Guided Intervention Strategy for Peripheral Lung Cancer. *Cancer Res.* **2016**, *76* (19), 5870−5880.
(172) Muhanna, N.; Jin, C. S.; Huynh, E.; Chan, H.; Qiu, Y.; Jiang, W.; Cui, L.; Burgess, L.; Akens, M. K.; Chen, J.; Irish, J. C.; Zheng, G. Phototheranostic Porphyrin Nanoparticles Enable Visualization and Targeted Treatment of Head and Neck Cancer in Clinically Relevant Models. *Theranostics* **2015**, *5* (12), 1428−43.
(173) Jin, C. S.; Lovell, J. F.; Chen, J.; Zheng, G. Ablation of hypoxic tumors with dose-equivalent photothermal, but not photodynamic, therapy using a nanostructured porphyrin assembly. *ACS Nano* **2013**, *7* (3), 2541−2550.
(174) Jin, C. S.; Overchuk, M.; Cui, L.; Wilson, B. C.; Bristow, R. G.; Chen, J.; Zheng, G. Nanoparticle-Enabled Selective Destruction of Prostate Tumor Using MRI-Guided Focal Photothermal Therapy. *Prostate* **2016**, *76* (13), 1169−81.
(175) Sheng, Z.; Hu, D.; Zheng, M.; Zhao, P.; Liu, H.; Gao, D.; Gong, P.; Gao, G.; Zhang, P.; Ma, Y.; Cai, L. Smart human serum albumin-indocyanine green nanoparticles generated by programmed assembly for dual-modal imaging-guided cancer synergistic phototherapy. *ACS Nano* **2014**, *8* (12), 12310−22.
(176) Harmatys, K. M.; Overchuk, M.; Zheng, G. Rational Design of Photosynthesis-Inspired Nanomedicines. *Acc. Chem. Res.* **2019**, *52* (5), 1265−1274.
(177) Ng, K. K.; Shakiba, M.; Huynh, E.; Weersink, R. A.; Roxin, A.; Wilson, B. C.; Zheng, G. Stimuli-responsive photoacoustic nanoswitch for in vivo sensing applications. *ACS Nano* **2014**, *8* (8), 8363−8373.
(178) Shakiba, M.; Ng, K. K.; Huynh, E.; Chan, H.; Charron, D. M.; Chen, J.; Muhanna, N.; Foster, F. S.; Wilson, B. C.; Zheng, G. Stable J-aggregation enabled dual photoacoustic and fluorescence nanoparticles for intraoperative cancer imaging. *Nanoscale* **2016**, *8* (25), 12618−25.
(179) Charron, D. M.; Yousefalizadeh, G.; Buzza, H. H.; Rajora, M. A.; Chen, J.; Stamplecoskie, K. G.; Zheng, G. Photophysics of J-Aggregating Porphyrin-Lipid Photosensitizers in Liposomes: Impact of Lipid Saturation. *Langmuir* **2020**, *36* (19), 5385−5393.
(180) Charron, D. M.; Chen, J.; Zheng, G. Nanostructure-dependent ratiometric NIR fluorescence enabled by ordered dye aggregation. *ChemNanoMat* **2016**, *2* (5), 430−436.
(181) Harmatys, K. M.; Chen, J.; Charron, D. M.; MacLaughlin, C. M.; Zheng, G. Multipronged Biomimetic Approach To Create Optically Tunable Nanoparticles. *Angew. Chem., Int. Ed. Engl.* **2018**, *57* (27), 8125−8129.
(182) Ng, K. K.; Weersink, R. A.; Lim, L.; Wilson, B. C.; Zheng, G. Controlling Spatial Heat and Light Distribution by Using Photothermal Enhancing Auto-Regulated Liposomes (PEARLs). *Angew. Chem., Int. Ed. Engl.* **2016**, *55* (34), 10003−7.
(183) Overchuk, M.; Zheng, M.; Rajora, M. A.; Charron, D. M.; Chen, J.; Zheng, G. Tailoring Porphyrin Conjugation for Nanoassembly-Driven Phototheranostic Properties. *ACS Nano* **2019**, *13* (4), 4560−4571.
(184) Zhao, H.; Xu, J.; Feng, C.; Ren, J.; Bao, L.; Zhao, Y.; Tao, W.; Zhao, Y.; Yang, X. Tailoring Aggregation Extent of Photosensitizers to Boost Phototherapy Potency for Eliciting Systemic Antitumor Immunity. *Adv. Mater.* **2021**, *34* (8), No. e2106390.
(185) Li, Y.; Lin, T. Y.; Luo, Y.; Liu, Q.; Xiao, W.; Guo, W.; Lac, D.; Zhang, H.; Feng, C.; Wachsmann-Hogiu, S.; Walton, J. H.; Cherry, S. R.; Rowland, D. J.; Kukis, D.; Pan, C.; Lam, K. S. A smart and versatile theranostic nanomedicine platform based on nanoporphyrin. *Nat. Commun.* **2014**, *5*, 4712.
(186) Zou, Q.; Abbas, M.; Zhao, L.; Li, S.; Shen, G.; Yan, X. Biological Photothermal Nanodots Based on Self-Assembly of Peptide-Porphyrin Conjugates for Antitumor Therapy. *J. Am. Chem. Soc.* **2017**, *139* (5), 1921−1927.
(187) Wang, D.; Zhang, Z.; Lin, L.; Liu, F.; Wang, Y.; Guo, Z.; Li, Y.; Tian, H.; Chen, X. Porphyrin-based covalent organic framework nanoparticles for photoacoustic imaging-guided photodynamic and photothermal combination cancer therapy. *Biomaterials* **2019**, *223*, 119459.
(188) Xue, X.; Huang, Y.; Bo, R.; Jia, B.; Wu, H.; Yuan, Y.; Wang, Z.; Ma, Z.; Jing, D.; Xu, X.; Yu, W.; Lin, T. Y.; Li, Y. Trojan Horse nanotheranostics with dual transformability and multifunctionality for highly effective cancer treatment. *Nat. Commun.* **2018**, *9* (1), 3653.
(189) Cong, Z.; Zhang, L.; Ma, S. Q.; Lam, K. S.; Yang, F. F.; Liao, Y. H. Size-Transformable Hyaluronan Stacked Self-Assembling Peptide Nanoparticles for Improved Transcellular Tumor Penetration and Photo-Chemo Combination Therapy. *ACS Nano* **2020**, *14* (2), 1958−1970.
(190) Gao, S.; Liu, Y.; Liu, M.; Yang, D.; Zhang, M.; Shi, K. Biodegradable mesoporous nanocomposites with dual-targeting function for enhanced anti-tumor therapy. *J. Controlled Release* **2022**, *341*, 383−398.
(191) Wang, K.; Zhang, Y.; Wang, J.; Yuan, A.; Sun, M.; Wu, J.; Hu, Y. Self-assembled IR780-loaded transferrin nanoparticles as an imaging, targeting and PDT/PTT agent for cancer therapy. *Sci. Rep* **2016**, *6*, 27421.
(192) Mei, H.; Zhang, X.; Cai, S.; Zhang, X.; Zhang, Y.; Guo, Z.; Shi, W.; Chu, R.; Zhang, K.; Cao, J.; He, B. Fluorocarbon-driven

https://doi.org/10.1021/acsnano.3c00891
ACS Nano 2023, 17, 7979−8003

photosensitizer assembly decodes energy conversion pathway for suppressing breast tumor. *Nano Today* **2021**, *41*, 101305.
(193) Zou, J.; Wang, P.; Wang, Y.; Liu, G.; Zhang, Y.; Zhang, Q.; Shao, J.; Si, W.; Huang, W.; Dong, X. Penetration depth tunable BODIPY derivatives for pH triggered enhanced photothermal/photodynamic synergistic therapy. *Chem. Sci.* **2019**, *10* (1), 268−276.
(194) He, H.; Ji, S.; He, Y.; Zhu, A.; Zou, Y.; Deng, Y.; Ke, H.; Yang, H.; Zhao, Y.; Guo, Z.; Chen, H. Photoconversion-Tunable Fluorophore Vesicles for Wavelength-Dependent Photoinduced Cancer Therapy. *Adv. Mater.* **2017**, *29* (19), 1606690.
(195) Chen, W.; Ouyang, J.; Liu, H.; Chen, M.; Zeng, K.; Sheng, J.; Liu, Z.; Han, Y.; Wang, L.; Li, J.; Deng, L.; Liu, Y. N.; Guo, S., Black Phosphorus Nanosheet-Based Drug Delivery System for Synergistic Photodynamic/Photothermal/Chemotherapy of Cancer. *Adv. Mater.* **2017**, *29* (5). DOI: 10.1002/adma.201603864.
(196) Jang, B.; Park, J. Y.; Tung, C. H.; Kim, I. H.; Choi, Y. Gold nanorod-photosensitizer complex for near-infrared fluorescence imaging and photodynamic/photothermal therapy in vivo. *ACS Nano* **2011**, *5* (2), 1086−94.
(197) Huang, X.; El-Sayed, I. H.; Qian, W.; El-Sayed, M. A. Cancer cell imaging and photothermal therapy in the near-infrared region by using gold nanorods. *J. Am. Chem. Soc.* **2006**, *128* (6), 2115−20.
(198) Peng, J.; Zhao, L.; Zhu, X.; Sun, Y.; Feng, W.; Gao, Y.; Wang, L.; Li, F. Hollow silica nanoparticles loaded with hydrophobic phthalocyanine for near-infrared photodynamic and photothermal combination therapy. *Biomaterials* **2013**, *34* (32), 7905−12.
(199) Jaque, D.; Martinez Maestro, L.; del Rosal, B.; Haro-Gonzalez, P.; Benayas, A.; Plaza, J. L.; Martin Rodriguez, E.; Garcia Sole, J. Nanoparticles for photothermal therapies. *Nanoscale* **2014**, *6* (16), 9494−530.
(200) Wen, K.; Wu, L.; Wu, X.; Lu, Y.; Duan, T.; Ma, H.; Peng, A.; Shi, Q.; Huang, H. Precisely Tuning Photothermal and Photodynamic Effects of Polymeric Nanoparticles by Controlled Copolymerization. *Angew. Chem., Int. Ed. Engl.* **2020**, *59* (31), 12756−12761.
(201) Wang, M.; Song, J.; Zhou, F.; Hoover, A. R.; Murray, C.; Zhou, B.; Wang, L.; Qu, J.; Chen, W. R. NIR-Triggered Phototherapy and Immunotherapy via an Antigen-Capturing Nanoplatform for Metastatic Cancer Treatment. *Adv. Sci. (Weinh)* **2019**, *6* (10), 1802157.
(202) Goel, S.; Ferreira, C. A.; Chen, F.; Ellison, P. A.; Siamof, C. M.; Barnhart, T. E.; Cai, W. Activatable Hybrid Nanotheranostics for Tetramodal Imaging and Synergistic Photothermal/Photodynamic Therapy. *Adv. Mater.* **2018**, *30* (6), 1704367.
(203) Feng, C. The Fabrication of Au Nanoparticles for Photocatalysis and Medical Applications: A Review. In *2022 8th International Conference on Mechanical Engineering and Automation Science (ICMEAS)*, Wuhan, China, Oct. 14−16, 2022; Institute of Electrical and Electronics Engineers: New York, 2022; pp 117−123.
(204) Bonet-Aleta, J.; Garcia-Peiro, J. I.; Hueso, J. L. Engineered Nanostructured Photocatalysts for Cancer Therapy. *Catalysts* **2022**, *12*, 167.
(205) He, L.; Mao, C.; Brasino, M.; Harguindey, A.; Park, W.; Goodwin, A. P.; Cha, J. N. TiO2-Capped Gold Nanorods for Plasmon-Enhanced Production of Reactive Oxygen Species and Photothermal Delivery of Chemotherapeutic Agents. *ACS Appl. Mater. Interfaces* **2018**, *10* (33), 27965−27971.
(206) Lin, J.; Wang, S.; Huang, P.; Wang, Z.; Chen, S.; Niu, G.; Li, W.; He, J.; Cui, D.; Lu, G.; Chen, X.; Nie, Z. Photosensitizer-loaded gold vesicles with strong plasmonic coupling effect for imaging-guided photothermal/photodynamic therapy. *ACS Nano* **2013**, *7* (6), 5320−9.
(207) Wang, S.; Huang, P.; Nie, L.; Xing, R.; Liu, D.; Wang, Z.; Lin, J.; Chen, S.; Niu, G.; Lu, G.; Chen, X. Single continuous wave laser induced photodynamic/plasmonic photothermal therapy using photosensitizer-functionalized gold nanostars. *Adv. Mater.* **2013**, *25* (22), 3055−61.
(208) Wu, F.; Liu, Y.; Wu, Y.; Song, D.; Qian, J.; Zhu, B. Chlorin e6 and polydopamine modified gold nanoflowers for combined photothermal and photodynamic therapy. *J. Mater. Chem. B* **2020**, *8* (10), 2128−2138.
(209) Kim, J. Y.; Choi, W. I.; Kim, M.; Tae, G. Tumor-targeting nanogel that can function independently for both photodynamic and photothermal therapy and its synergy from the procedure of PDT followed by PTT. *J. Controlled Release* **2013**, *171* (2), 113−21.
(210) Gong, B.; Shen, Y.; Li, H.; Li, X.; Huan, X.; Zhou, J.; Chen, Y.; Wu, J.; Li, W. Thermo-responsive polymer encapsulated gold nanorods for single continuous wave laser-induced photodynamic/photothermal tumour therapy. *J. Nanobiotechnology* **2021**, *19* (1), 41.
(211) Kuo, W. S.; Chang, Y. T.; Cho, K. C.; Chiu, K. C.; Lien, C. H.; Yeh, C. S.; Chen, S. J. Gold nanomaterials conjugated with indocyanine green for dual-modality photodynamic and photothermal therapy. *Biomaterials* **2012**, *33* (11), 3270−8.
(212) Younis, M. R.; Wang, C.; An, R.; Wang, S.; Younis, M. A.; Li, Z. Q.; Wang, Y.; Ihsan, A.; Ye, D.; Xia, X. H. Low Power Single Laser Activated Synergistic Cancer Phototherapy Using Photosensitizer Functionalized Dual Plasmonic Photothermal Nanoagents. *ACS Nano* **2019**, *13* (2), 2544−2557.
(213) Li, W.; Yang, J.; Luo, L.; Jiang, M.; Qin, B.; Yin, H.; Zhu, C.; Yuan, X.; Zhang, J.; Luo, Z.; Du, Y.; Li, Q.; Lou, Y.; Qiu, Y.; You, J. Targeting photodynamic and photothermal therapy to the endoplasmic reticulum enhances immunogenic cancer cell death. *Nat. Commun.* **2019**, *10* (1), 3349.
(214) Xing, R.; Liu, K.; Jiao, T.; Zhang, N.; Ma, K.; Zhang, R.; Zou, Q.; Ma, G.; Yan, X. An Injectable Self-Assembling Collagen-Gold Hybrid Hydrogel for Combinatorial Antitumor Photothermal/Photodynamic Therapy. *Adv. Mater.* **2016**, *28* (19), 3669−76.
(215) Tian, B.; Wang, C.; Zhang, S.; Feng, L.; Liu, Z. Photothermally enhanced photodynamic therapy delivered by nano-graphene oxide. *ACS Nano* **2011**, *5* (9), 7000−9.
(216) Sahu, A.; Choi, W. I.; Lee, J. H.; Tae, G. Graphene oxide mediated delivery of methylene blue for combined photodynamic and photothermal therapy. *Biomaterials* **2013**, *34* (26), 6239−48.
(217) Liu, T.; Wang, C.; Cui, W.; Gong, H.; Liang, C.; Shi, X.; Li, Z.; Sun, B.; Liu, Z. Combined photothermal and photodynamic therapy delivered by PEGylated MoS2 nanosheets. *Nanoscale* **2014**, *6* (19), 11219−25.
(218) Yang, X.; Wang, D.; Shi, Y.; Zou, J.; Zhao, Q.; Zhang, Q.; Huang, W.; Shao, J.; Xie, X.; Dong, X. Black Phosphorus Nanosheets Immobilizing Ce6 for Imaging-Guided Photothermal/Photodynamic Cancer Therapy. *ACS Appl. Mater. Interfaces* **2018**, *10* (15), 12431−12440.
(219) Morano, W. F.; Khalili, M.; Chi, D. S.; Bowne, W. B.; Esquivel, J. Clinical studies in CRS and HIPEC: Trials, tribulations, and future directions-A systematic review. *J. Surg Oncol* **2018**, *117* (2), 245−259.
(220) Liu, X.; Zhang, Y.; Wang, Y.; Zhu, W.; Li, G.; Ma, X.; Zhang, Y.; Chen, S.; Tiwari, S.; Shi, K.; Zhang, S.; Fan, H. M.; Zhao, Y. X.; Liang, X. J. Comprehensive understanding of magnetic hyperthermia for improving antitumor therapeutic efficacy. *Theranostics* **2020**, *10* (8), 3793−3815.
(221) Seynhaeve, A. L. B.; Amin, M.; Haemmerich, D.; van Rhoon, G. C.; Ten Hagen, T. L. M. Hyperthermia and smart drug delivery systems for solid tumor therapy. *Adv. Drug Deliv Rev.* **2020**, *163−164*, 125−144.
(222) Fu, X.; Cai, J.; Zhang, X.; Li, W. D.; Ge, H.; Hu, Y. Top-down fabrication of shape-controlled, monodisperse nanoparticles for biomedical applications. *Adv. Drug Deliv Rev.* **2018**, *132*, 169−187.
(223) Rao, J. P.; Geckeler, K. E. Polymer nanoparticles: Preparation techniques and size-control parameters. *Prog. Polym. Sci.* **2011**, *36* (7), 887−913.
(224) Hou, X.; Zaks, T.; Langer, R.; Dong, Y. Lipid nanoparticles for mRNA delivery. *Nat. Rev. Mater.* **2021**, *6* (12), 1078−1094.
(225) Leung, A. K.; Tam, Y. Y.; Chen, S.; Hafez, I. M.; Cullis, P. R. Microfluidic Mixing: A General Method for Encapsulating Macromolecules in Lipid Nanoparticle Systems. *J. Phys. Chem. B* **2015**, *119* (28), 8698−706.
(226) Karnik, R.; Gu, F.; Basto, P.; Cannizzaro, C.; Dean, L.; Kyei-Manu, W.; Langer, R.; Farokhzad, O. C. Microfluidic platform for controlled synthesis of polymeric nanoparticles. *Nano Lett.* **2008**, *8* (9), 2906−12.

(227) Li, B.; He, M.; Ramirez, L.; George, J.; Wang, J. Multifunctional Hydrogel Microparticles by Polymer-Assisted Photolithography. *ACS Appl. Mater. Interfaces* **2016**, *8* (6), 4158−64.
(228) Kim, D. H.; Rozhkova, E. A.; Ulasov, I. V.; Bader, S. D.; Rajh, T.; Lesniak, M. S.; Novosad, V. Biofunctionalized magnetic-vortex microdiscs for targeted cancer-cell destruction. *Nat. Mater.* **2010**, *9* (2), 165−71.
(229) Cook, A. B.; Clemons, T. D. Bottom-Up versus Top-Down Strategies for Morphology Control in Polymer-Based Biomedical Materials. *Advanced NanoBiomed Research* **2022**, *2* (1), 2100087.
(230) Huggett, M. T.; Jermyn, M.; Gillams, A.; Illing, R.; Mosse, S.; Novelli, M.; Kent, E.; Bown, S. G.; Hasan, T.; Pogue, B. W.; Pereira, S. P. Phase I/II study of verteporfin photodynamic therapy in locally advanced pancreatic cancer. *Br. J. Cancer* **2014**, *110* (7), 1698−704.
(231) Hanada, Y.; Pereira, S. P.; Pogue, B.; Maytin, E. V.; Hasan, T.; Linn, B.; Mangels-Dick, T.; Wang, K. K. EUS-guided verteporfin photodynamic therapy for pancreatic cancer. *Gastrointest Endosc* **2021**, *94* (1), 179−186.
(232) Damasco, J. A.; Ravi, S.; Perez, J. D.; Hagaman, D. E.; Melancon, M. P. Understanding Nanoparticle Toxicity to Direct a Safe-by-Design Approach in Cancer Nanomedicine. *Nanomaterials (Basel)* **2020**, *10* (11), 2186.
(233) Gnach, A.; Lipinski, T.; Bednarkiewicz, A.; Rybka, J.; Capobianco, J. A. Upconverting nanoparticles: assessing the toxicity. *Chem. Soc. Rev.* **2015**, *44* (6), 1561−84.
(234) Leong, H. S.; Butler, K. S.; Brinker, C. J.; Azzawi, M.; Conlan, S.; Dufes, C.; Owen, A.; Rannard, S.; Scott, C.; Chen, C.; Dobrovolskaia, M. A.; Kozlov, S. V.; Prina-Mello, A.; Schmid, R.; Wick, P.; Caputo, F.; Boisseau, P.; Crist, R. M.; McNeil, S. E.; Fadeel, B.; Tran, L.; Hansen, S. F.; Hartmann, N. B.; Clausen, L. P. W.; Skjolding, L. M.; Baun, A.; Agerstrand, M.; Gu, Z.; Lamprou, D. A.; Hoskins, C.; Huang, L.; Song, W.; Cao, H.; Liu, X.; Jandt, K. D.; Jiang, W.; Kim, B. Y. S.; Wheeler, K. E.; Chetwynd, A. J.; Lynch, I.; Moghimi, S. M.; Nel, A.; Xia, T.; Weiss, P. S.; Sarmento, B.; das Neves, J.; Santos, H. A.; Santos, L.; Mitragotri, S.; Little, S.; Peer, D.; Amiji, M. M.; Alonso, M. J.; Petri-Fink, A.; Balog, S.; Lee, A.; Drasler, B.; Rothen-Rutishauser, B.; Wilhelm, S.; Acar, H.; Harrison, R. G.; Mao, C.; Mukherjee, P.; Ramesh, R.; McNally, L. R.; Busatto, S.; Wolfram, J.; Bergese, P.; Ferrari, M.; Fang, R. H.; Zhang, L.; Zheng, J.; Peng, C.; Du, B.; Yu, M.; Charron, D. M.; Zheng, G.; Pastore, C. On the issue of transparency and reproducibility in nanomedicine. *Nat. Nanotechnol* **2019**, *14* (7), 629−635.
(235) Huynh, E.; Zheng, G. Engineering multifunctional nanoparticles: All-in-one versus one-for-all. *Wiley Interdisciplinary Reviews: Nanomedicine and Nanobiotechnology* **2013**, *5* (3), 250−265.
(236) Rawla, P.; Sunkara, T.; Gaduputi, V. Epidemiology of Pancreatic Cancer: Global Trends, Etiology and Risk Factors. *World J. Oncol* **2019**, *10* (1), 10−27.
(237) Bown, S. G.; Rogowska, A. Z.; Whitelaw, D. E.; Lees, W. R.; Lovat, L. B.; Ripley, P.; Jones, L.; Wyld, P.; Gillams, A.; Hatfield, A. W. Photodynamic therapy for cancer of the pancreas. *Gut* **2002**, *50* (4), 549−57.
(238) DeWitt, J. M.; Sandrasegaran, K.; O'Neil, B.; House, M. G.; Zyromski, N. J.; Sehdev, A.; Perkins, S. M.; Flynn, J.; McCranor, L.; Shahda, S. Phase 1 study of EUS-guided photodynamic therapy for locally advanced pancreatic cancer. *Gastrointest Endosc* **2019**, *89* (2), 390−398.
(239) Saccomandi, P.; Lapergola, A.; Longo, F.; Schena, E.; Quero, G. Thermal ablation of pancreatic cancer: A systematic literature review of clinical practice and pre-clinical studies. *Int. J. Hyperthermia* **2018**, *35* (1), 398−418.
(240) Guidolin, K.; Ding, L.; Yan, H.; Englesakis Hba, M.; Chadi, S.; Quereshy, F.; Zheng, G. Photodynamic Therapy for Colorectal Cancer: A Systematic Review of Clinical Research. *Surg Innov* **2022**, *29* (6), 788−803.
(241) Sun, B. O.; Li, W.; Liu, N. Curative effect of the recent photofrin photodynamic adjuvant treatment on young patients with advanced colorectal cancer. *Oncol Lett.* **2016**, *11* (3), 2071−2074.
(242) Vogl, T. J.; Eckert, R.; Naguib, N. N.; Beeres, M.; Gruber-Rouh, T.; Nour-Eldin, N. A. Thermal Ablation of Colorectal Lung Metastases: Retrospective Comparison Among Laser-Induced Thermotherapy, Radiofrequency Ablation, and Microwave Ablation. *AJR Am. J. Roentgenol* **2016**, *207* (6), 1340−1349.
(243) Vogl, T. J.; Farshid, P.; Naguib, N. N.; Darvishi, A.; Bazrafshan, B.; Mbalisike, E.; Burkhard, T.; Zangos, S. Thermal ablation of liver metastases from colorectal cancer: radiofrequency, microwave and laser ablation therapies. *Radiol Med.* **2014**, *119* (7), 451−61.
(244) Franckena, M.; Stalpers, L. J.; Koper, P. C.; Wiggenraad, R. G.; Hoogenraad, W. J.; van Dijk, J. D.; Warlam-Rodenhuis, C. C.; Jobsen, J. J.; van Rhoon, G. C.; van der Zee, J. Long-term improvement in treatment outcome after radiotherapy and hyperthermia in locoregionally advanced cervix cancer: an update of the Dutch Deep Hyperthermia Trial. *Int. J. Radiat Oncol Biol. Phys.* **2008**, *70* (4), 1176−82.

https://doi.org/10.1021/acsnano.3c00891
ACS Nano 2023, 17, 7979−8003